J Bone Miner Metab (2010) 28:627–633
DOI 10.1007/s00774-010-0179-y

ORIGINAL ARTICLE

Identification of oxytetracycline as a chondrogenic compound using a cell-based screening system

Hironori Hojo · Fumiko Yano · Shinsuke Ohba · Kazuyo Igawa · Keiji Nakajima · Yuske Komiyama · Akinori Kan · Toshiyuki Ikeda · Takayuki Yonezawa · Je-Tae Woo · Tsuyoshi Takato · Kozo Nakamura · Hiroshi Kawaguchi · Ung-il Chung

Received: 31 July 2009 / Accepted: 3 March 2010 / Published online: 8 April 2010

Abstract To effectively treat degenerative joint diseases including osteoarthritis (OA), small chemical compounds need to be developed that can potently induce chondrogenic differentiation without promoting terminal differentiation. For this purpose, we screened natural and synthetic compound libraries using a Col2GFP-ATDC5 system and identified oxytetracycline (Oxy) as a chondrogenic compound. Oxy induced cartilaginous matrix synthesis and mRNA expressions of chondrocyte markers in ATDC5 cells. In addition, Oxy suppressed mineralization and mRNA expressions of terminal chondrocyte differentiation markers in ATDC5 cells, primary chondrocytes, and cultured metatarsal bones. Oxy's induction of *Col2* mRNA expression was decreased by the addition of Noggin and was increased by the addition of BMP2. Furthermore, Oxy increased mRNA expression of *Id1*, *Bmp2*, *Bmp4*, and *Bmp6*. These data suggest that Oxy induces chondrogenic differentiation in a BMP-dependent manner and suppresses terminal differentiation. Oxy may be useful for treatment of OA and also for regeneration of cartilage tissue.

Keywords Small compound · Osteoarthritis · Chondrocyte differentiation · BMP · Col2GFP–ATDC5

Introduction

Degenerative joint diseases including osteoarthritis (OA) are common, particularly in the elderly. Early signs of OA include progressive loss of proteoglycan and aggrecan from articular cartilage and excessive damage to type 2 collagen (Col2), and general degeneration and fibrillation of the cartilage surface, resulting ultimately in a loss of articular cartilage [1]. Present treatments for this disease provide only transient relief from pain and do not repair the damaged articular cartilage. Therefore, novel drugs that regenerate articular cartilage are desired.

Chondrogenesis is an important biological event for endochondral bone development, skeletogenesis, and joint formation [2, 3]. The first step in chondrogenesis is the aggregation of mesenchymal cells into prechondrogenic condensations. These condensations differentiate into chondrocytes expressing cartilage-specific genes, such as transcriptional factor *Sox9* (sex-determining region Y-type high-mobility group box9), *Sox5*, *Sox6*, and chondrocyte collagen *Col2*, *Col9*, and *Col11*. In the growth plate,

Electronic supplementary material The online version of this article (doi:10.1007/s00774-010-0179-y) contains supplementary material, which is available to authorized users.

H. Hojo (✉) · F. Yano · S. Ohba · K. Igawa · K. Nakajima · Y. Komiyama · U. Chung (✉)
Center for Disease Biology and Integrative Medicine, Faculty of Medicine, University of Tokyo, 7-3-1 Hongo, Bunkyo-ku, Tokyo 113-0033, Japan
e-mail: hojo@bmw.t.u-tokyo.ac.jp

U. Chung
e-mail: tei@bioeng.t.u-tokyo.ac.jp

F. Yano · S. Ohba · K. Igawa · K. Nakajima · Y. Komiyama · A. Kan · T. Ikeda · T. Takato · K. Nakamura · H. Kawaguchi
Department of Sensory and Motor System Medicine, Faculty of Medicine, University of Tokyo, 7-3-1 Hongo, Bunkyo-ku, Tokyo 113-0033, Japan

T. Yonezawa · J.-T. Woo
Department of Nutriproteomics, Faculty of Medicine, University of Tokyo, 7-3-1 Hongo, Bunkyo-ku, Tokyo 113-0033, Japan

chondrocytes proliferate and further undergo terminal differentiation. During terminal differentiation, chondrocytes stop proliferating, enlarge (hypertrophy), and synthesize a specific cartilaginous matrix, such as *col10*. Hypertrophic chondrocytes direct the mineralization of their surrounding matrix, express specific markers, such as osteopontin (*Opn*) and matrix metalloproteinase 13 (*Mmp13*), attract blood vessels, and finally undergo apoptotic cell death. The cartilaginous matrix is then degraded and replaced by bone matrix. In contrast to the growth plate, which eventually undergoes endochondral ossification, articular cartilage is spared from terminal differentiation. The pathophysiological changes of the articular cartilage that occur in OA include the induction of terminal chondrocyte differentiation [4–6]. Therefore, to regenerate articular cartilage, it is necessary to induce chondrogenic differentiation without promoting terminal differentiation.

A number of factors have been shown to stimulate chondrogenic differentiation, such as Sox9 [7], insulin-like growth factor 1 (IGF-1) [8], bone morphogenetic proteins (BMPs) [9], transforming growth factors (TGFs) [10], and Wnt proteins [11]. These proteins were locally applied using direct protein delivery or viral gene delivery. Direct protein delivery, however, suffers from protein instability and inadequate post-translational modifications of the recombinant proteins [12]. As for viral gene delivery, their clinical use is severely limited due to the potential risk of immunogenic responses and the difficulty in manipulation and mass production.

Thus, there is a clear need for the development of small chondrogenic chemical compounds. For this purpose, we previously established the monitoring system of chondrogenic differentiation using Col2GFP-ATDC5 cells. Briefly, we established ATDC5 cells that were stably expressed with 4 tandem repeats of the COL2A1 enhancer region (+2,126/+2,174) cloned upstream of the COL2A1 basal promoter (−1,031/+37) in combination with the EGFP gene (called Col2GFP–ATDC5 cells). We confirmed that these cell lines showed time-dependent increases in the specific green fluorescence during the cultures, without being destroyed or fixed, and the fluorescence was enhanced by stimulation with insulin, a known chondrogenic stimulator of ATDC5 cells. This system allowed us to monitor the complex process of chondrogenic differentiation of living cells in real time without analyzing differentiation markers or staining the cells [13]. Using this system, we screened natural and synthetic compound libraries to identify the preeminent chondrogenic compound among them, and investigated its molecular mechanism using an in vitro and ex vivo culture system.

Materials and methods

Cell cultures

ATDC5 cells were obtained from the RIKEN BioResource Center Cell Bank (Tsukuba, Japan). Primary chondrocytes were isolated from WT C57BL/6N mice as described previously [14]. The ATDC5 cells were maintained in DMEM/Ham's F-12 (1:1) containing 5% fetal bovine serum (FBS, Sigma-Aldrich, St. Louis, MO) and 1% penicillin/streptomycin (Sigma-Aldrich). The primary chondrocytes were maintained in DMEM (Invitrogen, Carlsbad, CA) containing 10% fetal bovine serum (FBS, Sigma-Aldrich) and 1% penicillin/streptomycin (Sigma-Aldrich) (10% FBS/DMEM). To induce hypertrophic differentiation and mineralization, ATDC5 cells were cultured for 10 days, then the medium was replaced by α-MEM/5% FBS with 4 mM inorganic phosphate, and the cells were grown for 2 days, as described previously [15]. Toluidine blue staining and von Kossa staining were performed as described previously [7, 16].

Screening of small-compound libraries

In the first screening, 96-well plates (80 compounds tested per plate) were used to analyze 2,500 compounds. We treated Col2GFP-ATDC5 cells with each compound at 20 μg/ml for 6 days. Every 3 days, we observed GFP fluorescence. In the second screening, 24-well plates were used to analyze initial hit compounds. We treated Col2GFP-ATDC5 cells with each compound at 2 μg/ml for 7 days. We examined the cartilaginous matrix synthesis determined by toluidine blue staining. In the third screening, six-well plates were used to analyze hit compounds. We treated Col2GFP-ATDC5 cells with each compound at 2 μg/ml for 7 days. We examined the mRNA expression of *Col2* determined by real-time RT-PCR analysis.

Reagents and vectors

Oxytetracycline and Noggin/Fc chimeras were purchased from Sigma-Aldrich. The recombinant human (rh) BMP2 was provided by Astellas Pharma, Inc. (Tokyo, Japan). Small-compound libraries were purchased from InterBioScreen, Inc. (Chernogolovka, Russia). The plasmids expressing Smad1 and caALK6 were generous gifts of Dr. K. Miyazono (University of Tokyo), and the plasmid encoding 12xGCCG-luc a gift of Dr. T. Katagiri (Saitama Medical School). The plasmid expressing GFP was purchased from Clontech (Palo Alto, CA).

Real-time RT-PCR analysis

Total RNA was extracted using an ISOGEN Kit (Wako Pure Chemical Industries, Ltd., Tokyo, Japan) and treated with DNase I (Qiagen, Hilden, Germany) according to the manufacturer's instructions. After reverse-transcription using a Takara RNA PCR Kit (AMV) version 2.1 (Takara Shuzo Co., Shiga, Japan), PCR was performed with the ABI Prism 7000 Sequence Detection System (Applied Biosystems, Foster City, CA) using QuantiTect SYBR Green PCR Master Mix (Qiagen). All reactions were run in triplicate, and the mRNA copy number of a specific gene in the total RNA was calculated as described previously [17]. All data are expressed as means ± SDs of triplicate wells. The primer sequences are available upon request.

Metatarsal organ culture

Embryonic metatarsals were dissected and cultured as described previously [18]. The second, third, and fourth metatarsals from each embryonic (E15.5) hindlimb were dissected under sterile conditions. Each metatarsal was cultured in 1 ml of MEM (Invitrogen) supplemented with 50 μg/ml ascorbic acid, 1 mM β-glycerophosphate, and 0.25% fetal bovine serum in the presence or absence of oxytetracycline. These metatarsals were cultured at 37°C in a humidified 5% CO_2 incubator for 5 days.

Histological analysis

On day 5, cultured metatarsal rudiments were harvested and fixed in 4% paraformaldehyde/PBS overnight at 4°C, embedded in paraffin, and cut into 5-μm sections. Then von Kossa staining was performed as described previously [19]. In situ hybridization for *Col2*, *Col10*, *Opn*, and *Mmp13* was performed using DIG-labeled RNA probes as described previously [15].

Luciferase assay

The ATDC5 cells were plated onto 24-well plates and then transfected with 0.4 μg of a DNA mixture containing the test reporter plasmid, the control reporter plasmid encoding *Renilla* luciferase, and the effector plasmids using FuGene6 transfection reagent (Roche). After transfection, cells were incubated for 24 h followed by exposure to drugs for 48 h before cell harvest. The dual luciferase assay was performed as described previously [17]. All data were expressed as means ± SDs of triplicate wells.

Results

Identification of a chondrogenic compound, oxytetracycline

We screened natural and synthetic compound libraries using a Col2GFP-ATDC5 system. In the first screening, 65 initial hits were identified that induced GFP fluorescence. In the second screening, 20 hits were identified that induced cartilaginous matrix synthesis. In the third screening, 3 hits were identified that induced by more than twofold mRNA expression of *Col2*, which is one of the chondrogenic marker genes. Among them, oxytetracycline (Oxy) (Fig. 1a) was identified, which most strongly induced mRNA expression of *Col2* in ATDC5 cells (data not shown).

Therefore, we examined the chondrogenic effect of Oxy. We treated ATDC5 cells with Oxy at concentrations ranging from 0.01 to 10 μM for 10 days. As shown by toluidine blue staining, Oxy induced cartilaginous matrix synthesis in a dose-dependent manner (Fig. 1b). We then examined mRNA expression of the chondrogenic marker genes. Oxy induced mRNA expressions of chondrocyte collagens (*Col2*, *Col9*, *Col11*), and transcription factors regulating chondrogenesis (*Sox5, Sox6, Sox9*) in a dose-dependent manner (Fig. 1c). These data suggest that Oxy exerts a potent chondrogenic effect on ATDC5 cells. Oxy also induced mRNA expressions of chondrocyte collagens (*Col2*, *Col9*, *Col11*) in primary chondrocytes (Supplementary Fig. 1). On the other hand, Oxy did not induce chondrogenic differentiation of C3H10T1/2, a murine mesenchymal stem cell line, at 10 days (data not shown), suggesting that Oxy acts only on cells committed to the chondrocyte lineage.

Suppression of terminal chondrocyte differentiation by Oxy

We next examined the effects of Oxy on terminal chondrocyte differentiation. We used Oxy to treat ATDC5 cells cultured in differentiation medium including inorganic phosphate. Oxy reduced von Kossa staining and mRNA expressions of terminal chondrocyte differentiation markers, *Col10*, *Opn*, and *Mmp13* in a dose-dependent manner (Fig. 2a, b). Oxy also reduced *Col10*, *Opn, Mmp13* mRNA expressions in primary chondrocytes (Fig. 2c).

To investigate the effects of Oxy ex vivo, metatarsals were isolated and cultured with Oxy for 5 days. Terminal chondrocyte differentiation was analyzed by von Kossa staining and in situ hybridization. Oxy not only increased the size of regions expressing *Col2*, but also reduced the size of regions of mineralization and regions expressing

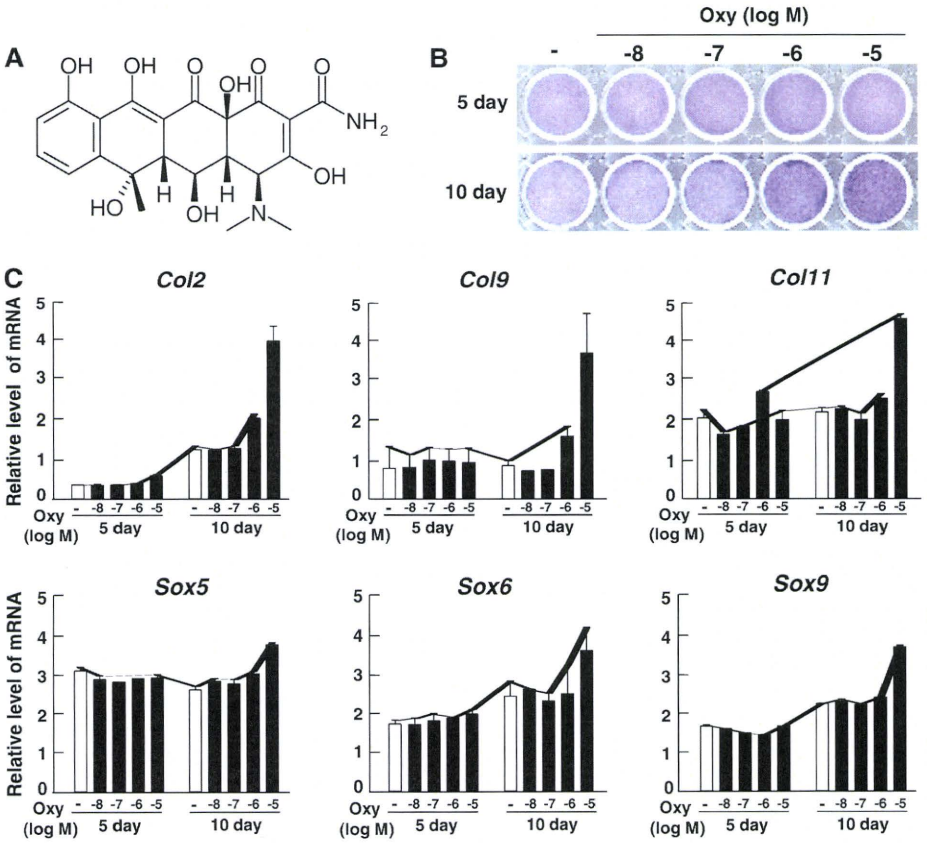

Fig. 1 Chondrogenic induction of ATDC5 cells by oxytetracycline (*Oxy*). **a** Chemical structure of Oxy. **b** Cartilaginous matrix synthesis of ATDC5 cells determined by toluidine blue staining. Cells were treated with Oxy for 10 days. **c** Expression of chondrogenic marker genes in ATDC5 cells determined by real-time RT-PCR analysis. Cells were treated with Oxy for 10 days. Data are expressed as means ± SDs of triplicate wells

Col10, *Opn*, and *Mmp13* in a dose-dependent manner (Fig. 3). These data suggest that Oxy suppresses terminal chondrocyte differentiation.

Involvement of BMP/Smad signaling in Oxy's chondrogenic effect

We next examined the involvement of major chondrogenic pathways in Oxy's effect. A luciferase assay using reporter plasmids driven by BMP-responsive elements (12xGCCG), TGFβ-responsive elements (9xCAGA), canonical-Wnt-responsive elements (TOPflash), and Hh-responsive elements (8 × 3′ Gli-BS) showed that Oxy stimulated BMP signaling pathways within 48 h (Fig. 4a), while Oxy did not significantly alter TGFβ, canonical-Wnt, or Hh signaling pathways (Supplementary Fig. 3). Oxy's induction of *Col2* mRNA expression was decreased by the addition of Noggin, a potent BMP antagonist, and was increased by the addition of BMP2 (Fig. 4b). In addition, Oxy increased mRNA expression of *Id1* (a transcriptional target of BMP signaling), *Bmp2, Bmp4,* and *Bmp6* (Fig. 4c). Furthermore, Oxy's induction of *Col2* mRNA expression was decreased by the transfection of siSox6, siSox9, and siBmp2 (Supplementary Fig. 2). These data suggest that induction of *Col2* mRNA expression by Oxy is mediated by Sox6, Sox9, and Bmp2.

Discussion

In this study, we screened natural and synthetic compound libraries using COL2GFP-ATDC5 cells and identified oxytetracycline (Oxy) as a chondrogenic compound that induces chondrocyte differentiation without promoting terminal differentiation. Some in vitro and in vivo studies suggest that several tetracycline analogs slow the progression of OA. In vitro studies have shown that tetracycline analogs reduced collagenase and gelatinase activity, which were associated with degradation of tissue matrices [20]. In vivo studies have shown that doxycycline (Dox), a structural homologue of Oxy, had a positive therapeutic effect in dogs with osteoarthritis in a 6-month clinical trial [21]. Dox significantly reduced levels of active and total gelatinase and collagenase in extracts of the OA cartilage in canines [22]. Furthermore, similar reductions in cartilage collagenase and gelatinase were obtained after administration of doxycycline to humans undergoing total joint arthroplasty [23]. These data may coincide with our data

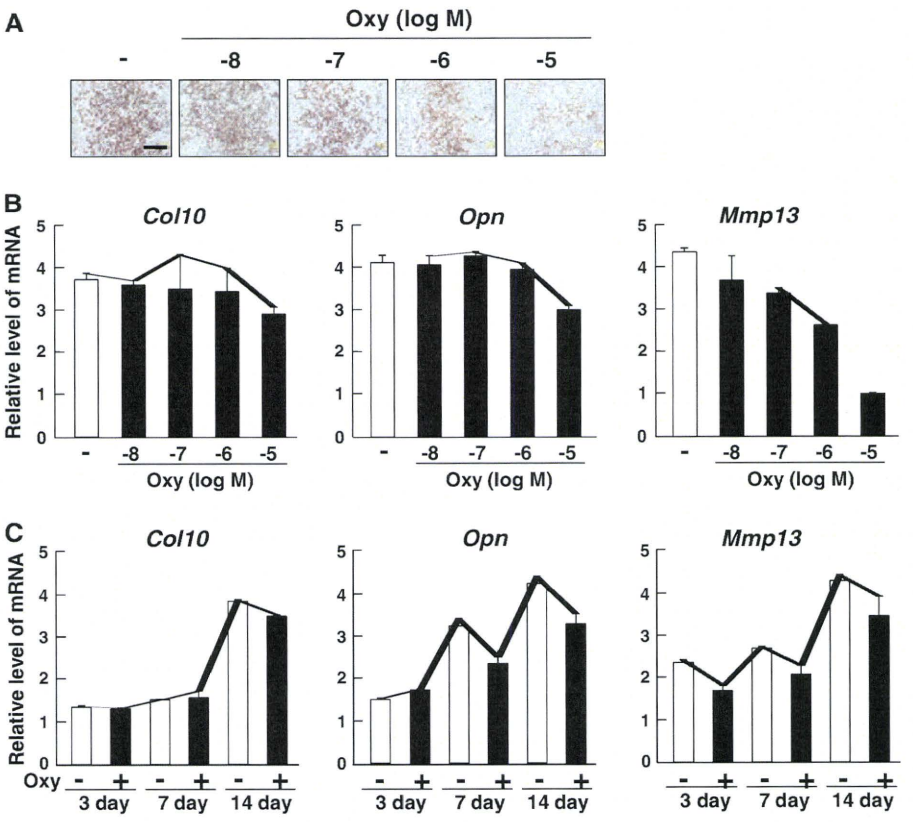

Fig. 2 Suppression of ATDC5 cells' terminal differentiation by Oxy. **a** Mineralization of ATDC5 cells was determined by von Kossa staining. Cells were cultured for 10 days with Oxy and for 2 days with inorganic phosphate and Oxy. *Scale bar* 200 μm. **b** mRNA expression of terminal chondrocyte differentiation marker genes in ATDC5 cells determined by real-time RT-PCR analysis. Cells were cultured for 10 days with Oxy and for 2 days with inorganic phosphate and Oxy. **c** Expression of terminal chondrocyte differentiation marker genes in primary chondrocytes determined by real-time RT-PCR analysis. Cells were treated with Oxy for 14 days. Data are expressed as means ± SDs of triplicate wells

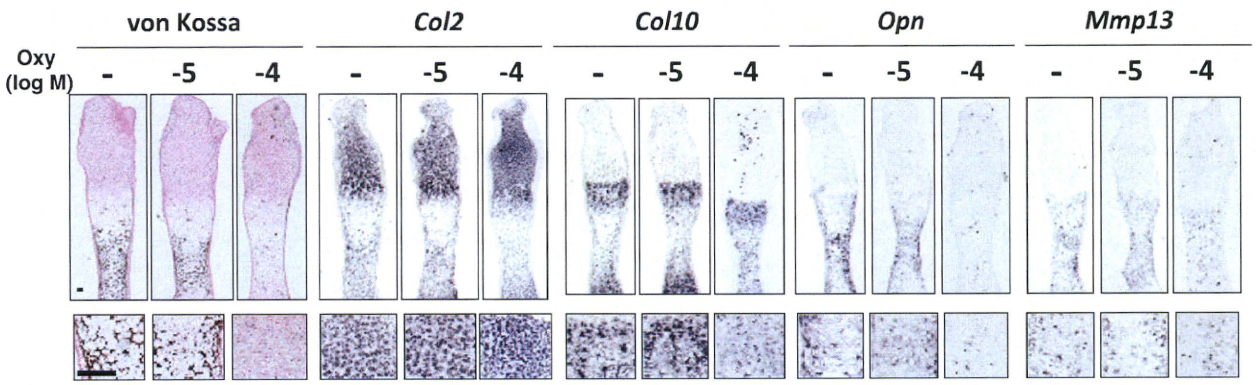

Fig. 3 Suppression of terminal chondrocyte differentiation of cultured metatarsals by Oxy. von Kossa staining and in situ hybridization of the sections from cultured metatarsals treated with Oxy for 5 days. *Scale bar* 100 μm

showing that Oxy suppressed terminal chondrocyte differentiation. In addition, we identified for the first time Oxy's action of inducing early chondrogenic differentiation. These data suggest that tetracycline analogs may be useful not only to slow the progression of OA, but also to regenerate cartilage tissues.

Oxy exerts its chondrogenic effect in a BMP-dependent manner. BMPs are known as potent stimulators of chondrogenesis and cartilage matrix synthesis of mesenchymal progenitor cells as well as terminal chondrocyte differentiation [24, 25]. Our data suggest that Oxy may indirectly activate BMP signaling through increasing expression of extracellular BMPs. However, Oxy and BMPs have opposite effects on terminal chondrocyte differentiation. These results suggest that other signaling pathways are likely to be involved in the inhibitory action of Oxy on terminal chondrocyte differentiation.

In summary, we identified Oxy as a chondrogenic compound that induces chondrocyte differentiation without promoting terminal differentiation. Oxy exerts its

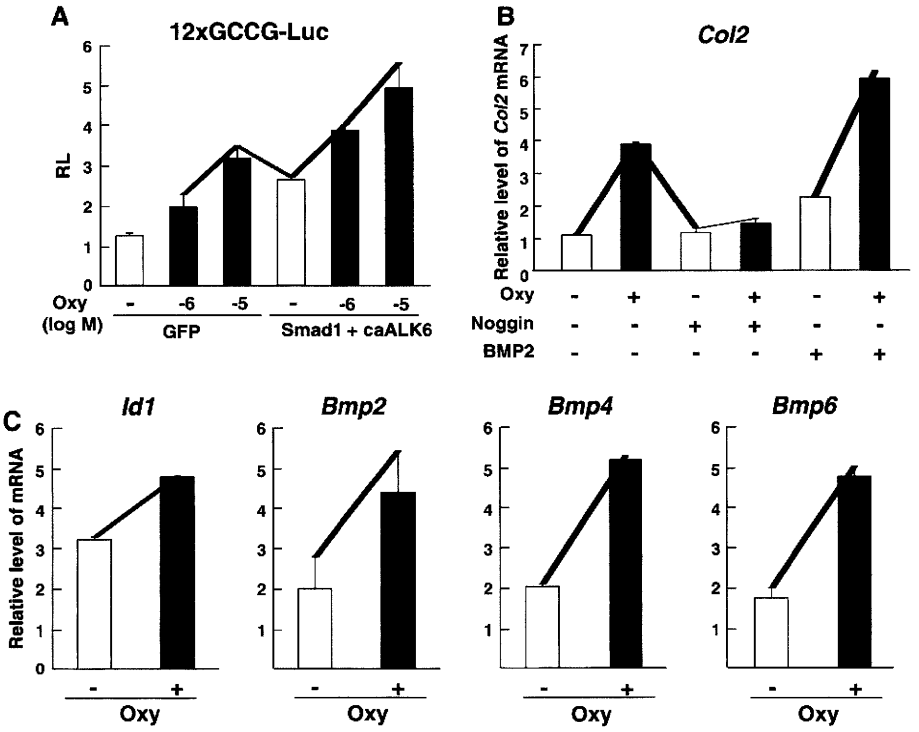

Fig. 4 Involvement of BMP signaling in Oxy's chondrogenic effect. **a** Luciferase reporter analysis of BMP signaling pathways. After being transfected with reporter constructs and the indicated effecter plasmids, ATDC5 cells were incubated for 24 h, followed by exposure to Oxy for 48 h. Luciferase activity was measured in cell lysates and normalized to the Renilla transfection control. **b** *Col2* mRNA expression of ATDC5 cells treated with Oxy (10 μM) in the presence or absence of Noggin (1 μg/ml) or rhBMP2 (200 ng/ml) determined by real-time RT-PCR analysis. **c** Expression of *Id1*, *Bmp2*, *Bmp4*, and *Bmp6* in ATDC5 cells determined by real-time RT-PCR analysis. Cells were cultured for 10 days with Oxy (10 μM). Data were expressed as means ± SDs of triplicate wells

chondrogenic effect in a BMP-dependent manner, partly through increasing expression of extracellular BMPs. Oxy may be useful for treatment of OA and also for regenerating cartilage tissue.

Acknowledgments We thank Drs. K. Miyazono, T. Katagiri, J. Y. Choi, A. Hecht, and H. Sasaki for their kind distribution of experimental materials, as well as Astellas Pharma, Inc., for providing rhBMP2. H. Hojo was supported by Research Fellowships from the Japan Society for the Promotion of Science for Young Scientists. This work was supported by Grants-in-Aid for Scientific Research from the Japanese Ministry of Education, Culture, Sports, Science and Technology (nos. 19390509 and 20390509).

References

1. Hollander AP, Pidoux I, Reiner A, Rorabeck C, Bourne R, Poole AR (1995) Damage to type II collagen in aging and osteoarthritis starts at the articular surface, originates around chondrocytes, and extends into the cartilage with progressive degeneration. J Clin Invest 96:2859–2869
2. Kronenberg HM (2003) Developmental regulation of the growth plate. Nature 423:332–336
3. Lefebvre V, Smits P (2005) Transcriptional control of chondrocyte fate and differentiation. Birth Defects Res C Embryo Today 75:200–212
4. Billinghurst RC, Dahlberg L, Ionescu M, Reiner A, Bourne R, Rorabeck C, Mitchell P, Hambor J, Diekmann O, Tschesche H, Chen J, Van Wart H, Poole AR (1997) Enhanced cleavage of type II collagen by collagenases in osteoarthritic articular cartilage. J Clin Invest 99:1534–1545
5. Pullig O, Weseloh G, Gauer S, Swoboda B (2000) Osteopontin is expressed by adult human osteoarthritic chondrocytes: protein and mRNA analysis of normal and osteoarthritic cartilage. Matrix Biol 19:245–255
6. Mitchell PG, Magna HA, Reeves LM, Lopresti-Morrow LL, Yocum SA, Rosner PJ, Geoghegan KF, Hambor JE (1996) Cloning, expression, and type II collagenolytic activity of matrix metalloproteinase-13 from human osteoarthritic cartilage. J Clin Invest 97:761–768
7. Ikeda T, Kamekura S, Mabuchi A, Kou I, Seki S, Takato T, Nakamura K, Kawaguchi H, Ikegawa S, Chung UI (2004) The combination of SOX5, SOX6, and SOX9 (the SOX trio) provides signals sufficient for induction of permanent cartilage. Arthritis Rheum 50:3561–3573
8. Kolettas E, Muir HI, Barrett JC, Hardingham TE (2001) Chondrocyte phenotype and cell survival are regulated by culture conditions and by specific cytokines through the expression of Sox-9 transcription factor. Rheumatology (Oxford) 40:1146–1156
9. Zehentner BK, Dony C, Burtscher H (1999) The transcription factor Sox9 is involved in BMP-2 signaling. J Bone Miner Res 14:1734–1741
10. Tuli R, Tuli S, Nandi S, Huang X, Manner PA, Hozack WJ, Danielson KG, Hall DJ, Tuan RS (2003) Transforming growth factor-beta-mediated chondrogenesis of human mesenchymal progenitor cells involves N-cadherin and mitogen-activated protein kinase and Wnt signaling cross-talk. J Biol Chem 278:41227–41236
11. Church VL, Francis-West P (2002) Wnt signalling during limb development. Int J Dev Biol 46:927–936
12. Fang J, Zhu YY, Smiley E, Bonadio J, Rouleau JP, Goldstein SA, McCauley LK, Davidson BL, Roessler BJ (1996) Stimulation of new bone formation by direct transfer of osteogenic plasmid genes. Proc Natl Acad Sci USA 93:5753–5758
13. Kan A, Ikeda T, Saito T, Yano F, Fukai A, Hojo H, Ogasawara T, Ogata N, Nakamura K, Chung UI, Kawaguchi H (2009)

Screening of chondrogenic factors with a real-time fluorescence-monitoring cell line ATDC5–C2ER: identification of sorting nexin 19 as a novel factor. Arthritis Rheum 60:3314–3323
14. Yano F, Kugimiya F, Ohba S, Ikeda T, Chikuda H, Ogasawara T, Ogata N, Takato T, Nakamura K, Kawaguchi H, Chung UI (2005) The canonical Wnt signaling pathway promotes chondrocyte differentiation in a Sox9-dependent manner. Biochem Biophys Res Commun 333:1300–1308
15. Saito T, Ikeda T, Nakamura K, Chung UI, Kawaguchi H (2007) S100A1 and S100B, transcriptional targets of SOX trio, inhibit terminal differentiation of chondrocytes. EMBO Rep 8:504–509
16. Ohba S, Ikeda T, Kugimiya F, Yano F, Lichtler AC, Nakamura K, Takato T, Kawaguchi H, Chung UI (2007) Identification of a potent combination of osteogenic genes for bone regeneration using embryonic stem (ES) cell-based sensor. FASEB J 21:1777–1787
17. Hojo H, Igawa K, Ohba S, Yano F, Nakajima K, Komiyama Y, Ikeda T, Lichtler AC, Woo JT, Yonezawa T, Takato T, Chung UI (2008) Development of high-throughput screening system for osteogenic drugs using a cell-based sensor. Biochem Biophys Res Commun 376:375–379
18. Wang L, Hinoi E, Takemori A, Nakamichi N, Yoneda Y (2006) Glutamate inhibits chondral mineralization through apoptotic cell death mediated by retrograde operation of the cystine/glutamate antiporter. J Biol Chem 281:24553–24565
19. Ohba S, Kawaguchi H, Kugimiya F, Ogasawara T, Kawamura N, Saito T, Ikeda T, Fujii K, Miyajima T, Kuramochi A, Miyashita T, Oda H, Nakamura K, Takato T, Chung UI (2008) Patched1 haploinsufficiency increases adult bone mass and modulates Gli3 repressor activity. Dev Cell 14:689–699
20. Yu LP Jr, Smith GN Jr, Hasty KA, Brandt KD (1991) Doxycycline inhibits type XI collagenolytic activity of extracts from human osteoarthritic cartilage and of gelatinase. J Rheumatol 18:1450–1452
21. Nganvongpanit K, Pothacharoen P, Suwankong N, Ong-Chai S, Kongtawelert P (2009) The effect of doxycycline on canine hip osteoarthritis: design of a 6-months clinical trial. J Vet Sci 10(3):239–247
22. Yu LP Jr, Smith GN Jr, Brandt KD, Myers SL, O'Connor BL, Brandt DA (1992) Reduction of the severity of canine osteoarthritis by prophylactic treatment with oral doxycycline. Arthritis Rheum 35:1150–1159
23. Smith GN Jr, Yu LP Jr, Brandt KD, Capello WN (1998) Oral administration of doxycycline reduces collagenase and gelatinase activities in extracts of human osteoarthritic cartilage. J Rheumatol 25:532–535
24. Yoon BS, Ovchinnikov DA, Yoshii I, Mishina Y, Behringer RR, Lyons KM (2005) Bmpr1a and Bmpr1b have overlapping functions and are essential for chondrogenesis in vivo. Proc Natl Acad Sci USA 102:5062–5067
25. Kobayashi T, Lyons KM, McMahon AP, Kronenberg HM (2005) BMP signaling stimulates cellular differentiation at multiple steps during cartilage development. Proc Natl Acad Sci USA 102:18023–18027

nature medicine

Transcriptional regulation of endochondral ossification by HIF-2α during skeletal growth and osteoarthritis development

Taku Saito[1,2], Atsushi Fukai[1], Akihiko Mabuchi[3], Toshiyuki Ikeda[2], Fumiko Yano[4], Shinsuke Ohba[4], Nao Nishida[3], Toru Akune[5], Noriko Yoshimura[5], Takumi Nakagawa[1], Kozo Nakamura[1], Katsushi Tokunaga[3], Ung-il Chung[4] & Hiroshi Kawaguchi[1]

Chondrocyte hypertrophy followed by cartilage matrix degradation and vascular invasion, characterized by expression of type X collagen (COL10A1), matrix metalloproteinase-13 (MMP-13) and vascular endothelial growth factor (VEGF), respectively, are central steps of endochondral ossification during normal skeletal growth and osteoarthritis development. A *COL10A1* promoter assay identified hypoxia-inducible factor-2α (HIF-2α, encoded by *EPAS1*) as the most potent transactivator of *COL10A1*. HIF-2α enhanced promoter activities of *COL10A1*, *MMP13* and *VEGFA* through specific binding to the respective hypoxia-responsive elements. HIF-2α, independently of oxygen-dependent hydroxylation, was essential for endochondral ossification of cultured chondrocytes and embryonic skeletal growth in mice. HIF-2α expression was higher in osteoarthritic cartilages versus nondiseased cartilages of mice and humans. *Epas1*-heterozygous deficient mice showed resistance to osteoarthritis development, and a functional single nucleotide polymorphism (SNP) in the human *EPAS1* gene was associated with knee osteoarthritis in a Japanese population. The *EPAS1* promoter assay identified RELA, a nuclear factor-κB (NF-κB) family member, as a potent inducer of HIF-2α expression. Hence, HIF-2α is a central transactivator that targets several crucial genes for endochondral ossification and may represent a therapeutic target for osteoarthritis.

Endochondral ossification is an essential process not only for physiological skeletal growth[1], but also for development of osteoarthritis, which is the most common joint disorder and is characterized by cartilage degradation and osteophyte formation[2–7]. The process of endochondral ossification requires both the hypertrophic differentiation of chondrocytes, which is characterized by secretion of COL10A1, and the conversion of avascular cartilage tissue into highly vascularized bone tissue via degradation of the cartilage matrix and vascular invasion[1,8]. The matrix degradation requires proteinases, among which MMP-13 has a major role[8,9], and the vascular invasion depends on an angiogenic switch by VEGF[8,10]. These steps of chondrocyte hypertrophy, cartilage degradation and vascular invasion are well coordinated; however, the molecular mechanism that extensively controls the sequential steps remains an enigma. Here we initially performed a screen of transcription factors that potentiate the expression of *COL10A1* and identify HIF-2α, an α-subunit member of the HIF family, as the most potent transactivator.

The HIF protein family consists of α- and β-subunit members that function by forming heterodimers[11]. Under normoxic conditions, the α-subunit members HIF-1α, HIF-2α and HIF-3α undergo oxygen-dependent hydroxylation, resulting in ubiquitination and degradation by the proteasome[12,13]. In contrast, under hypoxic conditions, they are neither hydroxylated nor degraded, and they heterodimerize with the constitutive β-subunit members known as aryl hydrocarbon receptor nuclear translocator (ARNT), ARNT2, ARNT-like (ARNTL) and ARNTL2. The heterodimers activate transcription of the target genes by binding the consensus sequence called hypoxia-responsive element (HRE) in the promoters[11]. As cartilage is an avascular and hypoxic tissue, HIF proteins may have a crucial role in the functions of chondrocytes, and, in fact, HIF-1α is known be a potent regulator of cartilage homeostasis[14–16]. However, HIF-2α and HIF-1α are not functionally redundant[17–21], and little is known about the function of HIF-2α in chondrocytes. Here we examined the role of HIF-2α in endochondral ossification during skeletal growth and osteoarthritis development and investigate the underlying mechanism.

RESULTS

Identification of HIF-2α as a transactivator of *COL10A1*

We initially performed a screen of transcription factors that induce hypertrophic differentiation using mouse chondrogenic ATDC5 cells and human nonchondrogenic HeLa cells transfected with a proximal promoter fragment of the *COL10A1* gene. For candidate molecules, we

[1]Sensory & Motor System Medicine, University of Tokyo, Hongo, Bunkyo-ku, Tokyo, Japan. [2]Bone and Cartilage Regenerative Medicine, University of Tokyo, Hongo, Bunkyo-ku, Tokyo, Japan. [3]Human Genetics, University of Tokyo, Hongo, Bunkyo-ku, Tokyo, Japan. [4]Center for Disease Biology and Integrative Medicine, University of Tokyo, Hongo, Bunkyo-ku, Tokyo, Japan. [5]22nd Century Medical and Research Center, Faculty of Medicine, University of Tokyo, Hongo, Bunkyo-ku, Tokyo, Japan. Correspondence should be addressed to H.K. (kawaguchi-ort@h.u-tokyo.ac.jp).

Received 10 February; accepted 8 March; published online 23 May 2010; doi:10.1038/nm.2146

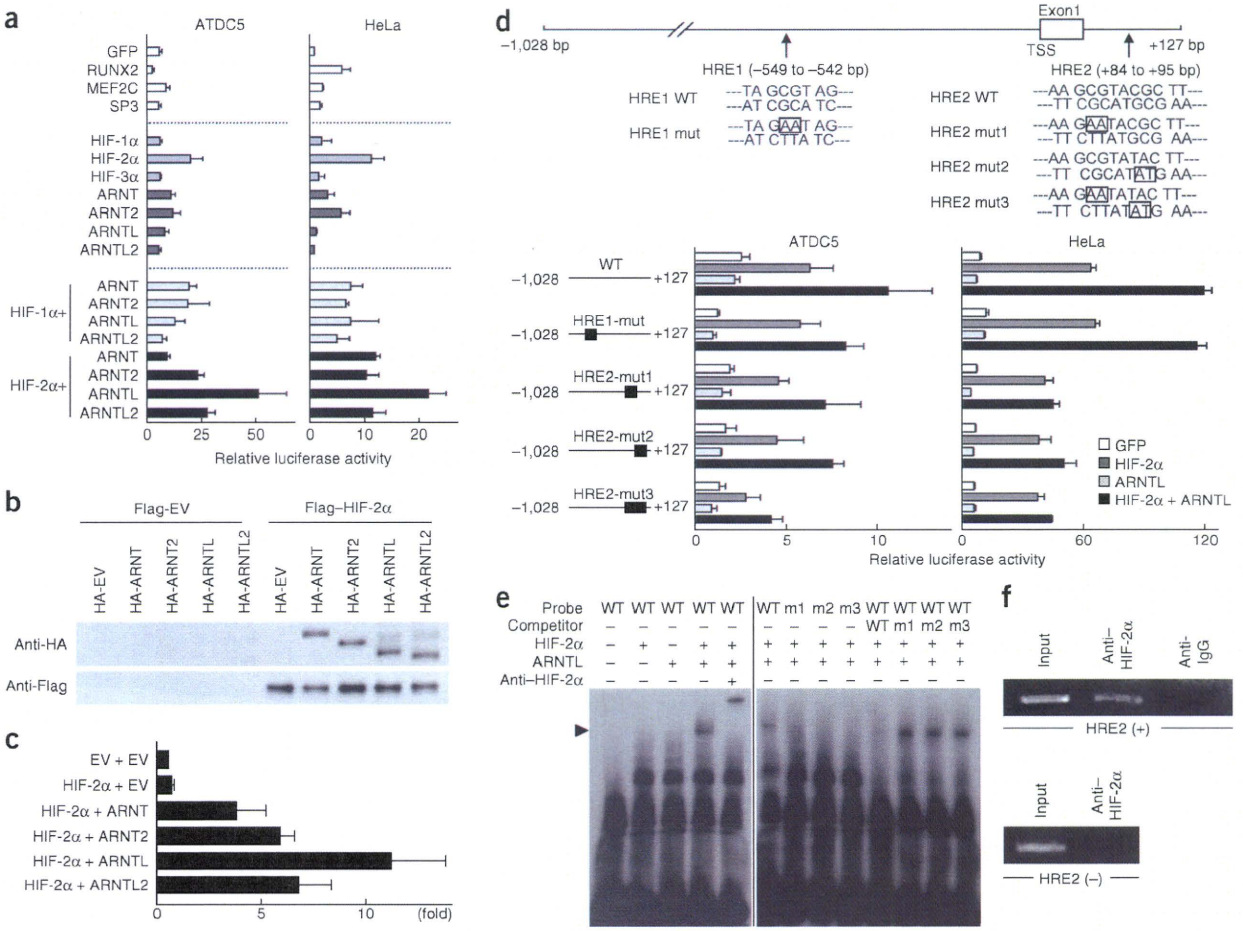

Figure 1 Transcriptional regulation of *COL10A1* by HIF-2α. (**a**) Luciferase assay for screening transcription factors that activate the *COL10A1* promoter by the transfections of candidate genes into ATDC5 and HeLa cells with a reporter construct containing a fragment (−1,028 to +127 bp) of the *COL10A1* gene. Data are shown as means ± s.d. (**b**) Immunoprecipitation and immunoblotting analysis by co-transfections of Flag-tagged HIF-2α or the control empty vector (EV) and hemagglutinin (HA)-tagged β-subunit members or the EV in ATDC5 cells. (**c**) Mammalian two-hybrid assay by transfections of vectors expressing GAL4–HIF-2α and VP16–β-subunit fusion proteins with the luciferase reporter vector with GAL4 binding sites into HeLa cells. Data are shown as means ± s.d. of relative fold increase in luciferase activity as compared to EV + EV (which is arbitrarily set to 1). (**d**) Site-directed mutagenesis analyses of the luciferase assay; one in HRE1 and three in HRE2 (+87 and +88 for mut1, +91 and +92 for mut2, and both for mut3), in the two cell lines transfected with GFP, HIF-2α, ARNTL or both HIF-2α and ARNTL. Data are shown as means ± s.d. (**e**) EMSA for specific binding (arrowhead) of the wild-type (WT) oligonucleotide probe containing HRE2 or the mutated probes described in **d** (m1, m2 and m3) with *in vitro*–translated HIF-2α, ARNT or both. Supershift by an antibody to HIF-2α (anti–HIF-2α) and cold competition with a 50-fold excess of unlabeled WT or the mutated probe are presented. (**f**) ChIP assay with cell lysates of human chondrogenic SW1353 cells that were amplified by a primer set spanning the HRE2 (+, +32 to +249 bp) or not spanning the HRE2 (−, −2,131 to −1,900 bp) before (input) and after immunoprecipitation with anti-HIF-2α or nonimmune IgG (anti-IgG).

prepared expression vectors of more than 100 transcription factors that are known to be expressed in chondrocytes, including HIF proteins, runt-related transcription factor-2 (RUNX2)[1,22], myocyte enhancer factor-2C (MEF2C)[23] and specificity protein-3 (SP3)[24] (**Fig. 1a**). Among them, HIF-2α showed the strongest activation in both cell lines. Although all β-subunit members were physically associated with HIF-2α in ATDC5 cells (**Fig. 1b**), ARNTL showed the strongest binding affinity to HIF-2α (**Fig. 1c**), and HIF-2α–ARNTL was the most potent combination for *COL10A1* transactivation (**Fig. 1a**).

In the *COL10A1* promoter, we identified two HREs by the consensus sequence [A/G]CGT (ref. 25), one in the 5′-end flanking region (HRE1) and the other in intron 1 (HRE2) (**Fig. 1d**). We introduced mutations in HRE1 and HRE2, but only the latter mutation resulted in suppression of transactivation by HIF-2α and the HIF-2α–ARNTL combination (**Fig. 1d**). We then confirmed the specific binding of the HIF-2α protein to HRE2 by electrophoretic mobility shift assay (EMSA) and chromatin immunoprecipitation (ChIP) assay (**Fig. 1e,f**).

HIF protein expression during chondrocyte differentiation

Although the HIF α- and β-subunit members were widely expressed in major tissues of adult mice, *Epas1* was most predominantly expressed in the tracheal cartilage (**Supplementary Fig. 1a**). During differentiation of ATDC5 cells, *Epas1* expression increased in accordance with the three representative factors for central steps of endochondral ossification: *Col10a1*, *Mmp13* and *Vegfa*, whereas *Hif1a* expression was strong at the early stage and decreased thereafter (**Fig. 2a**). *Hif3a* expression was very low, and the β-subunit members were extensively expressed in all differentiation stages (**Fig. 2a**).

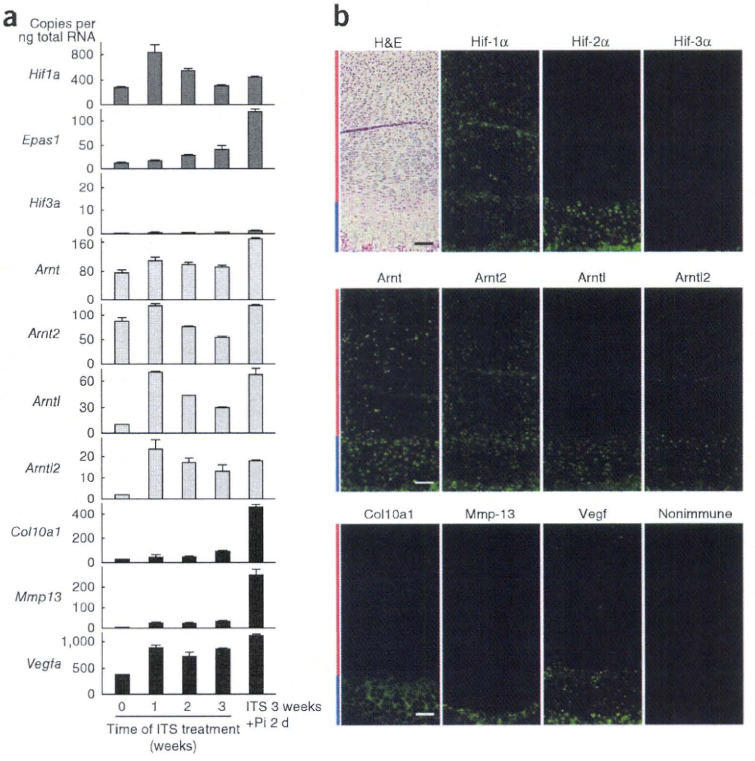

Figure 2 *In vitro* and *in vivo* expression patterns of the HIF α- and β-subunit members and Col10a1, Mmp-13 and Vegf during chondrocyte differentiation. (**a**) Time course of mRNA levels of the indicated genes during differentiation of mouse chondrogenic ATDC5 cells cultured with ITS (insulin, transferrin and sodium selenite) for 3 weeks and for 2 d more with inorganic phosphate (Pi). Data are expressed as means ± s.d. (**b**) H&E staining and immunofluorescence with antibodies to the indicated proteins, as well as a nonimmune control, in the proximal tibias of mouse embryos (embryonic day 18.5 (E18.5)). Scale bars, 100 μm. Red and blue bars to the left of each row indicate layers of proliferative and hypertrophic zones, respectively.

In tibial limb cartilage of mouse embryos, Hif-2α was localized primarily in the hypertrophic zone, similarly to Col10a1, Mmp-13 and Vegf (**Fig. 2b**). In contrast, Hif-1α was predominantly localized in chondrocytes at earlier differentiation stages in the proliferative zone, and Hif-3α was hardly detectable (**Fig. 2b**). The localizations of Arntl and Arntl2 were similar to Hif-2α, whereas those of Arnt and Arnt2 were similar to Hif-1α (**Fig. 2b**).

Physiological role of HIF-2α in endochondral ossification

To determine the involvement of HIF-2α in skeletal growth, we investigated the skeletal phenotype of *Epas1*-deficient mice. The homozygous deficient mutants (*Epas1*$^{-/-}$) were extraordinarily small and died at the early embryonic stage, as reported previously[20,21] (**Fig. 3a**). Although the heterozygous deficient mutants (*Epas1*$^{+/-}$) developed and grew without abnormalities of major organs, they showed mild but proportional dwarfism compared to wild-type littermates from embryonic stages up to 1 week after birth (**Fig. 3a,b** and **Supplementary Fig. 1b**). In the embryos, the limbs and vertebrae were 7–16% shorter in *Epas1*$^{+/-}$ mice than in the wild-type littermates (**Fig. 3c**). Although the actual length of the proliferative zone of the *Epas1*$^{+/-}$ limb was comparable to that of wild-type, the percentage of the proliferative zone relative to the total limb length was moderately increased (**Fig. 3d,e**) with normal BrdU-positive proliferative cells but suppressed Col10a1 expression (**Fig. 3f,g**), indicating impaired hypertrophic differentiation without an effect on proliferation caused by Hif-2α insufficiency. The percentage of the hypertrophic zone relative to the total limb length was also increased and that of the bone area was considerably decreased in the *Epas1*$^{+/-}$ limbs (**Fig. 3d,e**), indicating that Hif-2α insufficiency impaired not only chondrocyte hypertrophy but also subsequent steps such as matrix degradation and vascularization. This difference was gradually decreased with developmental compression of the hypertrophic zone after birth (**Supplementary Fig. 1c**). Immunohistochemistry confirmed that Mmp-13 and Vegf, as well as Col10a1, were suppressed by the Hif-2α insufficiency, which may cause the decrease in cartilage calcification shown by von Kossa staining (**Fig. 3f**).

Function of HIF-2α in cultured chondrocytes

In cultured ATDC5 cells, *Col10a1*, *Mmp13* and *Vegfa* amounts, as well as the activity of alkaline phosphatase and Alizarin red staining (both indicators of differentiation), were increased by overexpression of HIF-2α or the HIF-2α–ARNTL combination, whereas none of the expression levels or staining was affected by ARNTL alone (**Fig. 4a**). To examine the regulation of HIF-2α function by oxygen-dependent hydroxylation, we created ATDC5 lines overexpressing four kinds of HIF-2α mutants bearing mutations at the oxygen-dependent hydroxylation residues, including N847A and P531A (or both), which result in enhancement of the transactivation activity of the protein even under normoxic conditions, as well as P849A, which abrogates transactivation activity even under hypoxic conditions[13]. We found that none of these mutations affected the HIF-2α action on endochondral ossification parameters (**Fig. 4b**). All parameters were decreased, however, by loss of function of HIF-2α in ATDC5 cells achieved through overexpression of a dominant-negative mutant or expression of an siRNA specific for HIF-2α (**Fig. 4c**). In addition to ATDC cells, primary chondrocytes derived from *Epas1*$^{+/-}$ mice showed suppressed expression of the three factors, and the suppression of each factor was restored to wild-type levels by adenoviral overexpression of HIF-2α (**Fig. 4d**).

We then examined the transcriptional regulation of *MMP13* and *VEGFA* by HIF-2α. Among the α- and β-subunit members of the HIF proteins, HIF-2α most notably transactivated both *MMP13* and *VEGFA*, and the transactivation was further enhanced by ARNTL (**Supplementary Fig. 2a,b**), as is true for *COL10A1* (**Fig. 1a**). Deletion and site-directed mutagenesis analyses of the luciferase assay identified the core responsive elements to HIF-2α and the HIF-2α–ARNTL combination at HRE3 (−106 to −101) and HRE4 (−982 to −977) in the promoters of *MMP13* and *VEGFA*, respectively (**Supplementary Fig. 2c,d**). Further EMSA and ChIP assays confirmed the specific binding of the HIF-2α protein to HRE3 and HRE4 (**Supplementary Fig. 2e–h**).

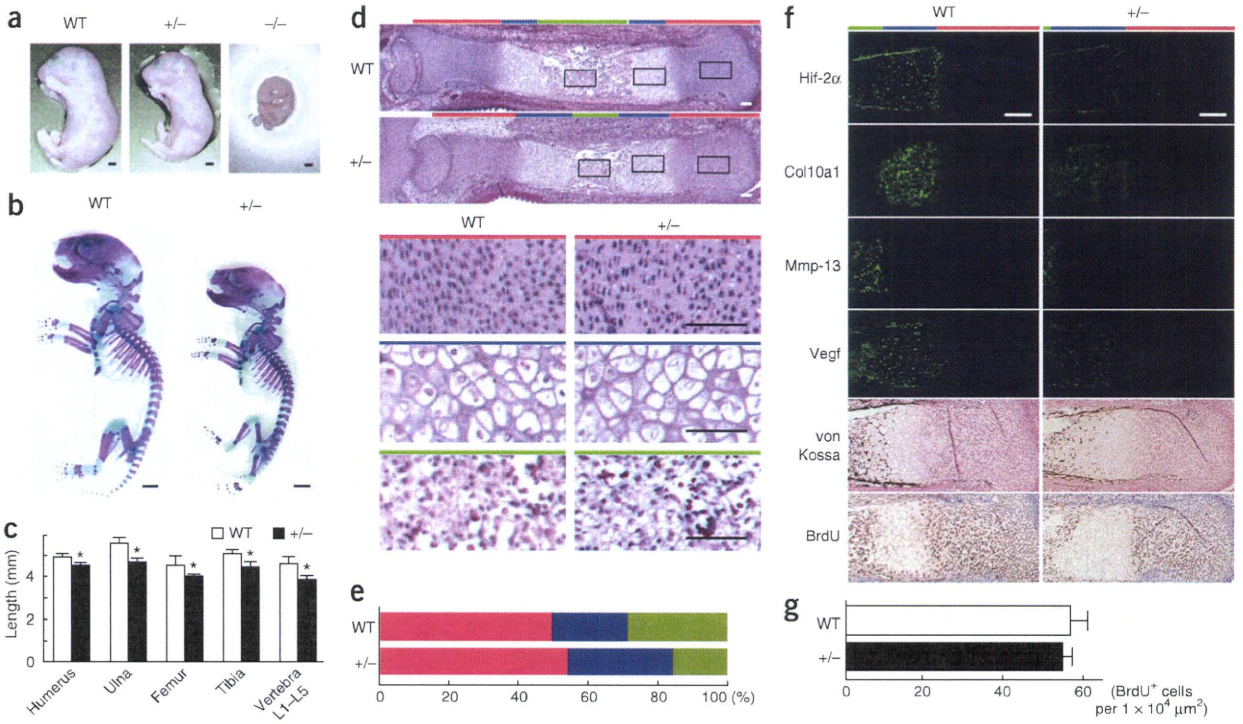

Figure 3 Skeletal abnormality in *Epas1*-deficient mice. (**a**) Wild-type (WT), heterozygous-deficient (*Epas1*$^{+/-}$) and homozygous-deficient (*Epas1*$^{-/-}$) littermate embryos (E17.5). All *Epas1*$^{-/-}$ embryos died at mid-gestation. Scale bars, 1 mm. (**b**) Double staining with Alizarin red and Alcian blue of the whole skeleton of WT and *Epas1*$^{+/-}$ littermate embryos (E17.5). Scale bars, 1 mm. (**c**) Length of long bones and vertebra (first to fifth lumbar spines) of WT and *Epas1*$^{+/-}$ littermate embryos. Data are expressed as means ± s.d. *$P < 0.05$ versus WT. (**d**) H&E staining of whole tibias of the WT and *Epas1*$^{+/-}$ littermate embryos. Inset boxes indicate the regions of the bottom three rows representing proliferative zone, hypertrophic zone and bone area, shown by red, blue and green bars, respectively. Scale bars, 100 μm. (**e**) Percentage of the length of proliferative zone (red), hypertrophic zone (blue) and bone area (green) over the total tibial length of the WT and *Epas1*$^{+/-}$ littermate embryos. (**f**) Immunofluorescence with antibodies to Hif-2α, Col10a1, Mmp-13 and Vegf, as well as bromodeoxyuridine (BrdU) labeling and von Kossa staining of the proximal tibias of WT and *Epas1*$^{+/-}$ littermate embryos (E17.5). Color bars indicate layers as indicated in **d**. Scale bars, 200 μm. (**g**) The number of BrdU-positive cells in 1 × 10^4 μm^2 of the proximal tibia of WT and *Epas1*$^{+/-}$ littermate embryos. Data are expressed as means ± s.d.

Contribution of HIF-2α to osteoarthritis in mice and humans

We next compared osteoarthritis development between adult littermates of wild-type and *Epas1*$^{+/-}$ mice that had undergone comparable skeletal growth after birth (**Supplementary Fig. 1b**) by creating a surgical osteoarthritis model through induction of instability to the knee joints[4,5]. The expression of Hif-2α, as well as of Col10a1, Mmp-13 and Vegf, increased in the joint cartilage with osteoarthritis development for 8 weeks after surgery in the wild-type mice; however, in the *Epas1*$^{+/-}$ littermates, the cartilage degradation and the expression of the three factors were notably suppressed (**Fig. 5a**). Quantification by grading systems[4,26] confirmed that the Hif-2α insufficiency caused significant resistance to cartilage degradation and osteophyte formation (**Fig. 5b**). There was no difference in the subchondral bones between the two genotypes under the sham operation, suggesting that the *Epas1* deficiency does not affect physiological bone homeostasis. However, after surgical induction, subchondral bone sclerosis, an osteoarthritic disorder secondary to cartilage destruction, was apparent in the wild-type joints, whereas it was suppressed in the *Epas1*$^{+/-}$ joints (**Supplementary Table 1**).

In human knee joint samples, as well, the HIF-2α expression increased with osteoarthritis development, reached a maximum at the initial and progressive stages and decreased thereafter at the terminal stage, although it was hardly detected in subchondral bone or synovium (**Fig. 5c**). To further investigate a possible association of the human *EPAS1* gene with knee osteoarthritis of humans, we searched a Japanese population–based cohort of the ROAD study[27] for sequence variations in exons and the 5′-end flanking region up to −1,000 bp from the transcription start site (TSS) of the human *EPAS1* gene and identified only one common SNP with a minor allele frequency >0.1, rs17039192 (+18C and +18T for major and minor alleles, respectively, relative to the TSS; minor allele frequency = 0.132) (**Fig. 5d**). A comparison of allelic frequencies between 397 individuals with knee osteoarthritis and 437 controls showed significant association of the rs17039192 SNP with knee osteoarthritis ($P = 0.013$, odds ratio = 1.44) (**Fig. 5d**). Because this SNP was located close to the TSS, we further examined the effects of the allelic difference (+18C/T) on *EPAS1* promoter activity in chondrogenic and nonchondrogenic cells transfected with a luciferase reporter gene and the *EPAS1* promoter fragment (−1,000 bp to 488 bp) containing +18C or +18T. The susceptibility allele (18C) showed higher promoter activity in chondrogenic cells, but not in nonchondrogenic cells (**Fig. 5e**), confirming that enhanced transactivation of *EPAS1* in chondrocytes is associated with osteoarthritis in humans.

Molecular network around HIF-2α in endochondral ossification

Regarding downstream molecules of HIF-2α, we have focused on COL10A1, MMP-13 and VEGF as representative factors for the

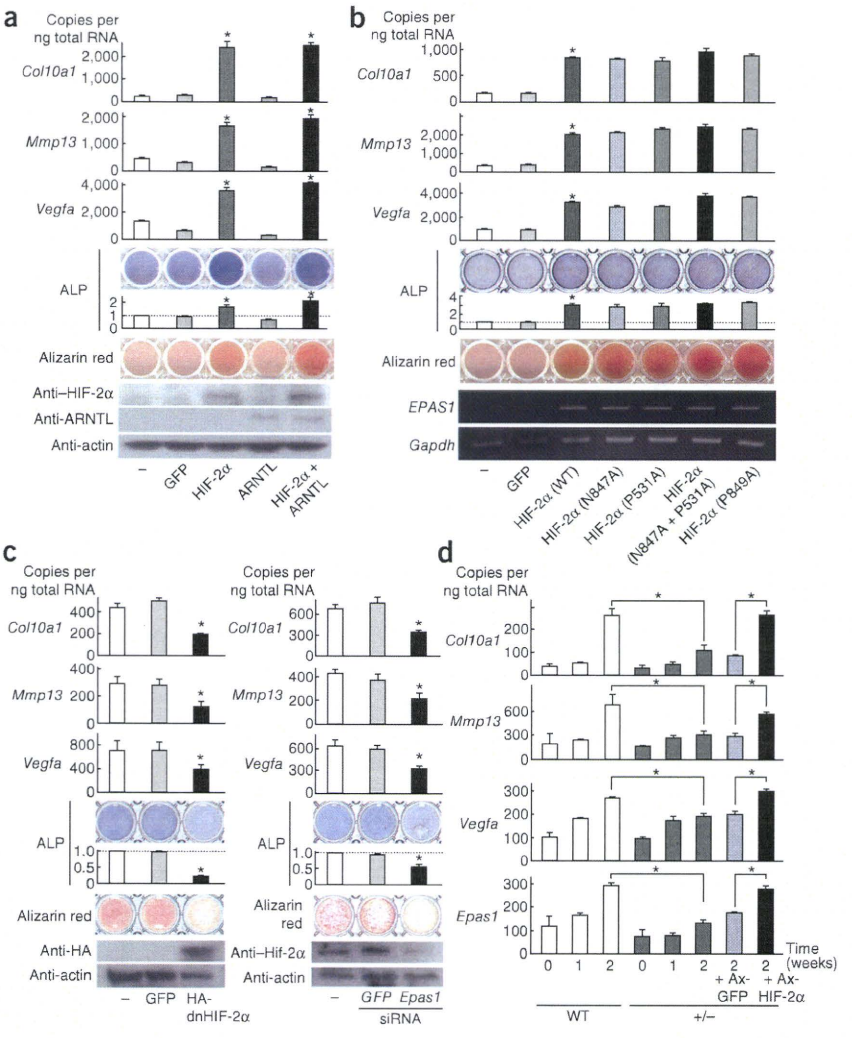

Figure 4 Effects of gain and loss of function of HIF-2α on endochondral ossification parameters in cultures of chondrogenic cells. (**a**) mRNA levels of *Col10a1*, *Mmp13* and *Vegfa*, alkaline phosphatase (ALP) activity (relative to control) and Alizarin red staining in stable lines of ATDC5 cells retrovirally transfected with GFP, HIF-2α, ARNTL or both HIF-2α and ARNTL and in nontransfected parental cells (–) after culture for 3 weeks with ITS and 2 d with Pi. HIF-2α and ARNTL levels were confirmed by western blotting, with the actin level as the internal control. (**b**) Analyses of the parameters in **a** in stable ATDC5 lines transfected with GFP or HIF-2α mutants at the oxygen-dependent hydroxylation residues causing enhancement (N847A and P531A) and abrogation (P849A) of HIF-2α transactivation activity under the culture conditions used in **a**. Gene expression was confirmed by RT-PCR with the *EPAS1* primer set inside the coding sequence, with the *Gapdh* level as the internal control. (**c**) Analyses of the same read-outs in **a** in stable ATDC5 lines transfected with GFP or HA-tagged dominant-negative HIF-2α (HA–dnHIF-2α) (left) or siRNA specific for *GFP* or *Epas1* mRNA (right) under the cultures conditions used in **a**. HA–dnHIF-2α and Hif-2α amounts were confirmed by western blotting. (**d**) mRNA levels of *Col10a1*, *Mmp13* and *Vegfa* and *Epas1* in the pellet cultures of primary chondrocytes derived from wild-type (WT) and *Epas1*$^{+/-}$ littermate embryos for 2 weeks. For the rescue experiment, adenoviral transfection with HIF-2α (Ax–HIF-2α) or the control GFP (Ax-GFP) was performed before the pellet formation. All data are expressed as means ± s.d. $^*P < 0.05$ versus GFP unless otherwise indicated.

central three steps of endochondral ossification (chondrocyte hypertrophy, cartilage degradation and vascularization) and found that all were the direct transcriptional targets. However, there are other factors related to endochondral ossification, including in the earlier cartilage formation step and in the later osteogenesis step, which might also be targets of HIF-2α. We therefore examined the expression patterns of the following factors: type II collagen (COL2A1) and aggrecan (AGC1) as cartilage matrix proteins; RUNX2, Indian hedgehog (IHH), and type 1 PTH/PTHrP receptor (PTH1R) as chondrocyte hypertrophy markers; MMP-3, MMP-9, a disintegrin and metalloproteinase with thrombospondin type 1 motif-4 (ADAMTS4) and ADAMTS5 as cartilage-degradable proteinases; and type I collagen (COL1A1), bone sialoprotein (BSP), osteocalcin, alkaline phosphatase, bone morphogenetic protein-2 (BMP-2), BMP-4 and BMP-7 as osteogenic markers. In cultured ATDC5 cells, expression of chondrocyte hypertrophy markers, cartilage degradable proteinases and osteogenic markers increased in accordance with the cell differentiation and *Epas1* expression (**Supplementary Fig. 3a**). The chondrocyte hypertrophy markers and cartilage degradable proteinases were localized mainly in the hypertrophic zone of the mouse limb cartilage, similarly to Hif-2α (**Supplementary Fig. 3b**). The mRNA levels of cartilage matrix proteins, chondrocyte hypertrophy markers and most of the osteogenic markers were increased in ATDC5 cells overexpressing HIF-2α or HIF-2α–ARNTL (**Supplementary Fig. 4a**). Among cartilage-degradable proteinases, expression of *Mmp3* and *Mmp9* was increased, whereas neither *Adamts4* nor *Adamts5* was affected (**Supplementary Fig. 4a**). In contrast, mRNA levels of the chondrocyte hypertrophy markers *Mmp3* and *Mmp9* were decreased after overexpression of a dominant-negative mutant form of HIF-2α and siRNA specific for *Epas1* mRNA in ATDC5 cells (**Supplementary Fig. 4b,c**); however, cartilage matrix proteins, *Adamts4*, *Adamts5* and most of osteogenic markers were little affected. Primary chondrocytes derived from *Epas1*$^{+/-}$ mice reproducibly showed suppression of the chondrocyte hypertrophy markers, *Mmp3* and *Mmp9*, but not cartilage matrix proteins, *Adamts4*, *Adamts5* or osteogenic factors, and the suppression was restored to wild-type levels by HIF-2α overexpression (**Supplementary Fig. 5**). Further *in vivo* analyses of embryonic limbs (**Supplementary Fig. 6a**) and osteoarthritic knee joints (**Supplementary Fig. 6b**) confirmed the decreases in expression of the chondrocyte hypertrophy markers, Mmp-3 and Mmp-9, but not cartilage matrix proteins Adamts4 or Adamts5, by Hif-2α insufficiency. HIF-2α enhanced the promoter activities of the chondrocyte hypertrophy markers *MMP3* and *MMP9*, as well as *Col10a1*, *Mmp13*, and *Vegfa* mRNA levels, much more strongly than HIF-1α, and the stimulation of the mRNA levels by HIF-2α was not altered by cotransfection of

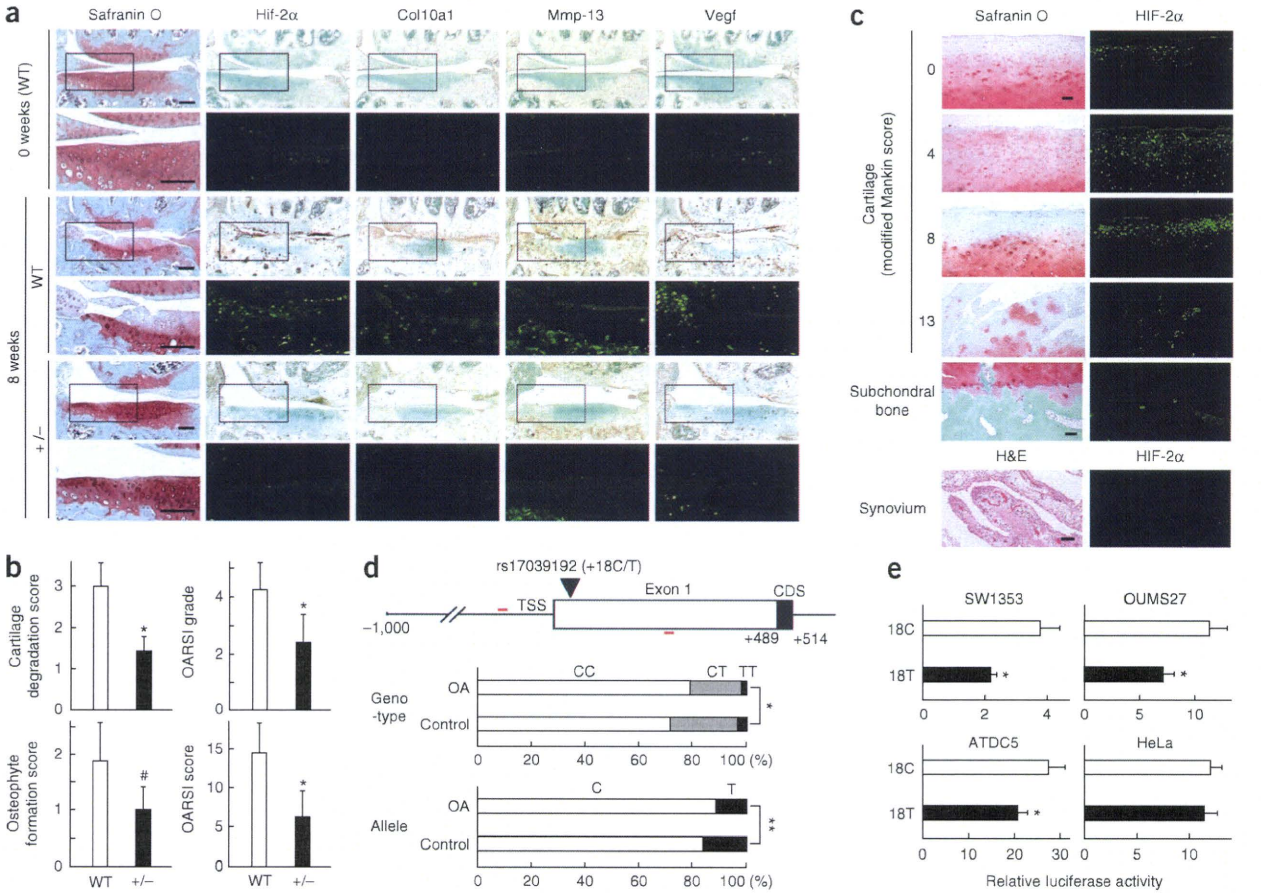

Figure 5 Contribution of HIF-2α to osteoarthritis development in mice and humans. (**a**) Cartilage degradation assessed by safranin O staining and expression of Hif-2α, Col10a1, Mmp-13 and Vegf by immunostaining (brown) and immunofluorescence (green) in mouse knee joints 0 and 8 weeks after creating a surgical osteoarthritis model in 8-week-old wild-type (WT) and *Epas1*$^{+/-}$ littermates. Boxed areas in each safranin O–stained or each immunostained image indicate the regions shown in the enlarged safranin O–stained or immunofluorescent image immediately below. Scale bars, 100 μm. (**b**) Quantification of osteoarthritis development by our (two left graphs) and OARSI (two right graphs) grading systems. Data are expressed as means ± s.d. #$P < 0.05$, *$P < 0.01$ versus WT. (**c**) Safranin O staining, H&E staining and immunofluorescence with an antibody to HIF-2α in human tibial cartilages of various degradation stages, subchondral bone (beneath the cartilage with Mankin score = 8) and synovium (around the cartilage with Mankin score = 8), obtained as surgical specimens of total knee arthroplasty. Scale bars, 100 μm. (**d**) Top, the identified SNP, rs17039192, and primers used for genotyping (red lines) in the human *EPAS1* gene. CDS, coding sequence. Bottom, association of the rs17039192 (+18C/T) SNP with knee osteoarthritis (OA) diagnosed on radiographs using the Kellgren/Lawrence grade in a Japanese population. The odds ratio of the susceptibility allele was 1.44 (95% confidence interval: 1.08–1.92). *$P = 0.05$, **$P = 0.013$. (**e**) Luciferase activities in chondrogenic SW1353, OUMS27 and ATDC5 cells and nonchondrogenic HeLa cells transfected with a luciferase reporter gene construct ligated to a fragment (−1,000 bp to +488 bp) containing +18C or +18T. Data are shown as means ± s.d. *$P < 0.05$ versus 18C.

HIF-1α (**Supplementary Fig. 7a,b**). Furthermore, the endochondral ossification parameters stimulated by HIF-2α overexpression in ATDC5 cells were not inhibited by suppression of RUNX2 through overexpression of a dominant-negative mutant RUNX2 (**Supplementary Fig. 7c**).

Finally, to identify the upstream mechanism that regulates HIF-2α, we performed a screen of transcription factors with the *EPAS1* promoter fragment including the +18C SNP described above. Among candidate molecules that are known to regulate chondrocyte differentiation, such as sex-determining region Y box (SOX), RUNX, CCAAT/enhancer binding protein (C/EBP), MEF2, SP/Kruppel-like factor (KLF), activating transcription factor (ATF), cAMP responsive element–binding protein (CREB), Notch and NF-κB family members, we found that v-rel reticuloendotheliosis viral oncogene homolog A (RELA or NF-κB p65), an essential molecule of the NF-κB signal, showed the strongest activation in all cells (**Fig. 6a**). In the *EPAS1* promoter we identified an NF-κB motif and found that site-directed mutagenesis in the motif caused suppression of transactivation by RELA (**Fig. 6b**). The allelic difference (+18C/T) of the rs17039192 SNP described above also altered the activation of *EPAS1* promoter by RELA but did not affect it when the NF-κB motif was mutated, suggesting the involvement of this SNP in the *EPAS1* transactivation and osteoarthritis development caused by the NF-κB signal. We further confirmed that the proinflammatory cytokines tumor necrosis factor-α (TNF-α) and interleukin-1β (IL-1β), putative inducers of the NF-κB signal[28], increased *EPAS1* expression in cultured chondrogenic cells (**Fig. 6c**). In mouse knee joint cartilage, the expression of Rela was increased during osteoarthritis development, similarly to Hif-2α expression (**Fig. 6d**).

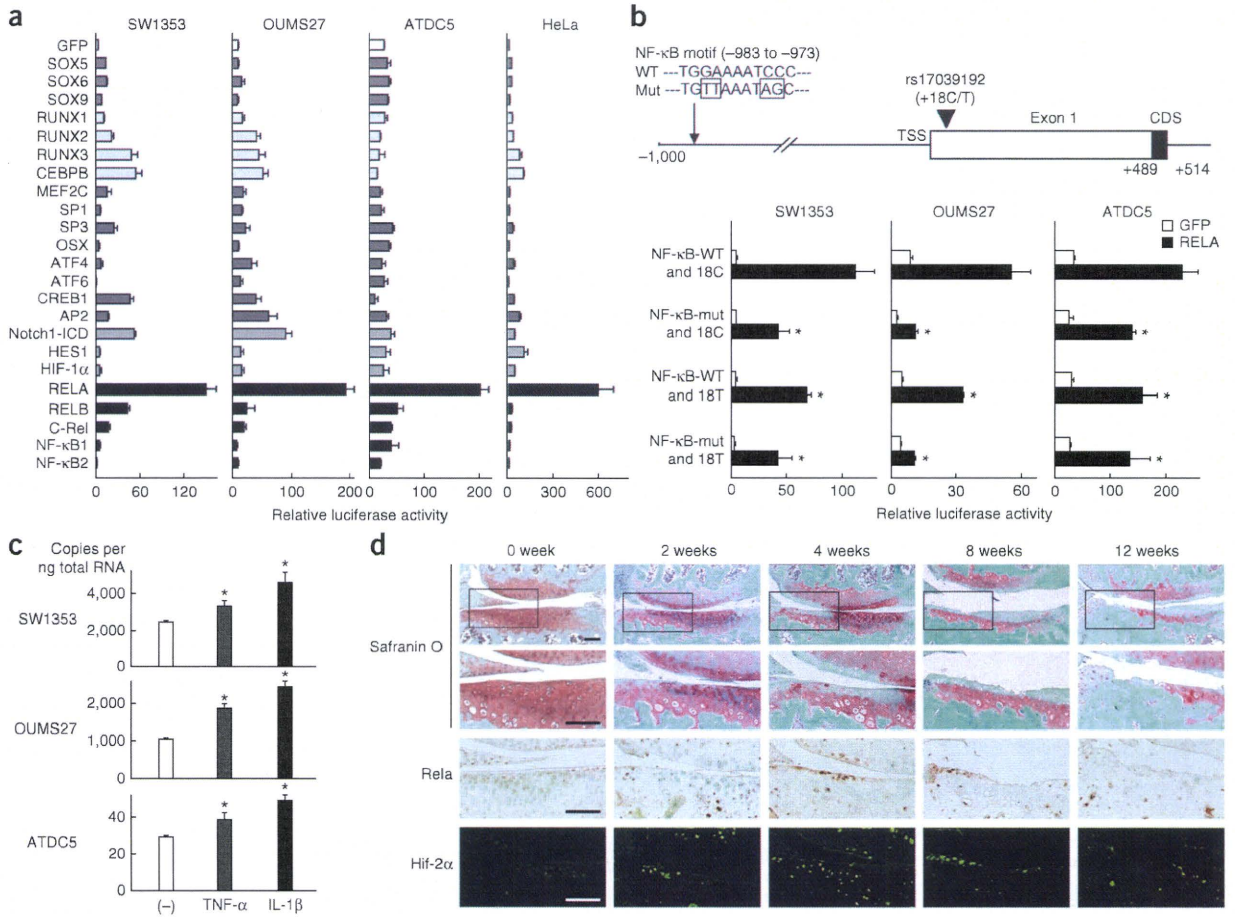

Figure 6 Upstream mechanism that regulates HIF-2α. (**a**) Luciferase activities after transfections of putative chondrocyte-related transcription factors into chondrogenic SW1353, OUMS27 and ATDC5 cells and nonchondrogenic HeLa cells with a reporter construct containing a fragment (–1,000 bp to +488 bp) of the *EPAS1* gene. OSX, osterix; AP2, transcription factor AP-2α; Notch1-ICD, intercellular domain of Notch1; HES1, hairy and enhancer of split 1. Data are shown as means ± s.d. (**b**) Top, depiction of the NF-κB motif (–983 to –973) in the human *EPAS1* gene. Bottom, site-directed mutagenesis analyses of the luciferase assay in the three chondrogenic cell lines transfected with GFP or RELA. Luciferase activities were compared with or without mutation in the NF-κB motif and with +18C or +18T of the rs17039192 SNP. Data are shown as means ± s.d. $^*P < 0.05$ versus wild-type NF-κB and 18C with RELA. (**c**) mRNA levels of *EPAS1* in the three chondrogenic cells cultured with or without TNF-α or IL-1β (each 1 ng ml^{-1}) for 2 d. Data are expressed as means ± s.d. $^*P < 0.05$ versus control. (**d**) Time course of degradation in mouse knee joint cartilage, as shown by Safranin O staining and expression of Rela and Hif-2α by immunostaining and immunofluorescence, respectively, in a surgical osteoarthritis model in 8-week-old mice. Boxed areas in each of the top images are enlarged in the bottom images directly beneath. Scale bar, 100 μm.

DISCUSSION

Among the sequential steps of endochondral ossification—cartilage formation, chondrocyte hypertrophy, cartilage degradation, vascularization and osteogenesis—this study reveals that HIF-2α functions as an extensive transcriptional regulator of the central three steps. HIF-2α shares about 50% amino acid homology with HIF-1α (ref. 20), a potent regulator of cartilage homeostasis[14–16]; however, accumulating evidence has shown distinct expression patterns and functions between the two HIF proteins[17–21]. HIF-1α is expressed mainly in hypovascular and hypoxic tissues[16,19,29], whereas HIF-2α is expressed even in vascularized tissues[11,29]. In cartilage as well, previous studies and our current study show that HIF-1α is expressed from the early stage of cartilage formation, and its activity is enhanced by hypoxia[13–16,30]. In contrast, HIF-2α is expressed mainly in highly differentiated chondrocytes, and its function is independent of oxygen-dependent hydroxylation. Likewise, although cartilage-specific knockout of HIF-1α leads to defects in the earlier stage of cartilage formation and the later stage of chondrocyte survival and osteogenesis[14–16], *Epas1*$^{+/-}$ mice show growth retardation with defects in the central steps of endochondral ossification. Hence, HIF-1α and HIF-2α may have distinct roles via different mechanisms: hypoxia-dependent cartilage formation and maintenance by HIF-1α and less hypoxia-dependent endochondral ossification by HIF-2α. We have also confirmed that neither gain nor loss of function of HIF-2α alters HIF-1α expression during chondrocyte differentiation, nor does HIF-1α transfection affect *EPAS1* promoter activity. Furthermore, HIF-1α hardly stimulates the expression of markers of the central steps of endochondral ossification in the presence or absence of HIF-2α, indicating independent functions of HIF-1α and HIF-2α at least in the central steps. However, we do not deny the possibility of interactions between HIF-1α and HIF-2α in earlier and later stages of endochondral ossification. The HIF-2α function may possibly be compensated by HIF-1α in this earlier stage, as cartilage matrix proteins are not altered by HIF-2α suppression. In the later or severe stage of osteoarthritic

cartilage, expression of HIF-2α decreases after reaching a maximum at the initiation of cartilage degradation in mice and humans, as was reported in a previous study[31]. In this terminal stage, the decreased HIF-2α expression may enhance autophagy in mature chondrocytes of osteoarthritic cartilage, as HIF-2α is known to antagonize the autophagy-accelerator function of HIF-1α[32].

Our study reveals that *COL10A1*, *MMP13* and *VEGFA* are the direct transcriptional targets of HIF-2α. The functional relationships *in vivo* are supported by previous reports that a deficiency of *Mmp13* or *Vegfa* in mice causes a skeletal phenotype similar to that in *Epas1*$^{+/-}$ mice, with elongation of the hypertrophic zone and delay of ossification in the limb cartilage[9,10], although the skeletal phenotypes of *Col10a1*-knockout mice differs among the reports[33–35]. Our further studies identify *RUNX2*, *IHH*, *PTH1R*, *MMP3* and *MMP9* as possible transcriptional targets of HIF-2α. We have recently reported that HIF-2α enhances *Runx2* promoter activity[36] and that *Runx2*$^{+/-}$ mice show resistance to osteoarthritis development under mechanical instability, similarly to *Epas1*$^{+/-}$ mice[5]. However, HIF-2α and RUNX2 may promote endochondral ossification via independent mechanisms.

There are two mechanisms of osteoarthritis protection: induction of anabolism or inhibition of catabolism in joint cartilage. The protection in *Epas1*$^{+/-}$ mice is not likely to be due to induction of anabolism, as the anabolic markers COL2A1 and AGC1 are unaffected in joint cartilage. Although recent studies have identified ADAMTS5 and related molecules as key catabolic regulators of osteoarthritis development[37–40], neither ADAMTS4 nor ADAMTS5 is regulated by HIF-2α, implicating another pathway. Because *Mmp13*$^{-/-}$ mice are reported to be protected from cartilage degradation despite considerable aggrecan loss after surgical osteoarthritis induction[41], similarly to *Epas1*$^{+/-}$ mice, the osteoarthritis protection caused by the Hif-2α insufficiency might occur principally through regulation of Mmp-13.

Suppression of osteoarthritis development was obvious in *Epas1*$^{+/-}$ mice, whereas skeletal growth retardation was mild and transient, suggesting that pathological endochondral ossification is more dependent on HIF-2α than is physiological endochondral ossification. As a trigger of osteoarthritis, mechanical stress may induce the upstream NF-κB signal and HIF-2α expression in joint cartilage, which causes endochondral ossification by transactivation of *COL10A1*, *MMP13*, *VEGFA* and other factors. Recent comprehensive profiling analyses of not only genes and proteins, but also microRNAs, is unraveling the molecular network underlying osteoarthtitis development[42]; however, we hereby propose that signals in the HIF-2α axis from NF-κB signaling to endochondral ossification–related molecules may represent a rational therapeutic target for osteoarthritis with minimal effects on physiological skeletal homeostasis.

METHODS

Methods and any associated references are available in the online version of the paper at http://www.nature.com/naturemedicine/.

Note: Supplementary information is available on the Nature Medicine website.

ACKNOWLEDGMENTS

We thank R. Yamaguchi and H. Kawahara for technical assistance. This study was supported by a grant-in-aid for Scientific Research from the Japanese Ministry of Education, Culture, Sports, Science and Technology (19109007 and 20689028). The sponsor had no role in study design, data collection, data analysis, data interpretation or writing of the manuscript.

AUTHOR CONTRIBUTIONS

T.S., T.I. and H.K. performed project planning; T.S., A.F., A.M., F.Y. and S.O. performed the experiments; T.S., A.M., N.N., T.A., N.Y., T.N., K.N., K.T., U.-i.C. and H.K. conducted data analysis; T.S. and H.K. wrote the manuscript.

COMPETING FINANCIAL INTERESTS

The authors declare no competing financial interests.

Published online at http://www.nature.com/naturemedicine/.
Reprints and permissions information is available online at http://npg.nature.com/reprintsandpermissions/.

1. Kronenberg, H.M. Developmental regulation of the growth plate. *Nature* **423**, 332–336 (2003).
2. Kühn, K., D'Lima, D.D., Hashimoto, S. & Lotz, M. Cell death in cartilage. *Osteoarthritis Cartilage* **12**, 1–16 (2004).
3. Kawaguchi, H. Endochondral ossification signals in cartilage degradation during osteoarthritis progression in experimental mouse models. *Mol. Cells* **25**, 1–6 (2008).
4. Kamekura, S. *et al.* Osteoarthritis development in novel experimental mouse models induced by knee joint instability. *Osteoarthritis Cartilage* **13**, 632–641 (2005).
5. Kamekura, S. *et al.* Contribution of runt-related transcription factor 2 to the pathogenesis of osteoarthritis in mice after induction of knee joint instability. *Arthritis Rheum.* **54**, 2462–2470 (2006).
6. Yamada, T. *et al.* Carminerin contributes to chondrocyte calcification during endochondral ossification. *Nat. Med.* **12**, 665–670 (2006).
7. Drissi, H., Zuscik, M., Rosier, R. & O'Keefe, R. Transcriptional regulation of chondrocyte maturation: potential involvement of transcription factors in OA pathogenesis. *Mol. Aspects Med.* **26**, 169–179 (2005).
8. Ortega, N., Behonick, D.J. & Werb, Z. Matrix remodeling during endochondral ossification. *Trends Cell Biol.* **14**, 86–93 (2004).
9. Stickens, D. *et al.* Altered endochondral bone development in matrix metalloproteinase 13–deficient mice. *Development* **131**, 5883–5895 (2004).
10. Zelzer, E. *et al.* VEGFA is necessary for chondrocyte survival during bone development. *Development* **131**, 2161–2171 (2004).
11. Semenza, G.L. HIF-1 and human disease: one highly involved factor. *Genes Dev.* **14**, 1983–1991 (2000).
12. Schofield, C.J. & Ratcliffe, P.J. Oxygen sensing by HIF hydroxylases. *Nat. Rev. Mol. Cell Biol.* **5**, 343–354 (2004).
13. Lando, D., Peet, D.J., Whelan, D.A., Gorman, J.J. & Whitelaw, M.L. Asparagine hydroxylation of the HIF transactivation domain a hypoxic switch. *Science* **295**, 858–861 (2002).
14. Pfander, D., Cramer, T., Schipani, E. & Johnson, R.S. HIF-1α controls extracellular matrix synthesis by epiphyseal chondrocytes. *J. Cell Sci.* **116**, 1819–1826 (2003).
15. Schipani, E. Hypoxia and HIF-1α in chondrogenesis. *Ann. NY Acad. Sci.* **1068**, 66–73 (2006).
16. Schipani, E. *et al.* Hypoxia in cartilage: HIF-1α is essential for chondrocyte growth arrest and survival. *Genes Dev.* **15**, 2865–2876 (2001).
17. Patel, S.A. & Simon, M.C. Biology of hypoxia-inducible factor-2α in development and disease. *Cell Death Differ.* **15**, 628–634 (2008).
18. O'Rourke, J.F., Tian, Y.M., Ratcliffe, P.J. & Pugh, C.W. Oxygen-regulated and transactivating domains in endothelial PAS protein 1: comparison with hypoxia-inducible factor-1α. *J. Biol. Chem.* **274**, 2060–2071 (1999).
19. Jain, S., Maltepe, E., Lu, M.M., Simon, C. & Bradfield, C.A. Expression of ARNT, ARNT2, HIF1 α, HIF2 α and Ah receptor mRNAs in the developing mouse. *Mech. Dev.* **73**, 117–123 (1998).
20. Tian, H., Hammer, R.E., Matsumoto, A.M., Russell, D.W. & McKnight, S.L. The hypoxia-responsive transcription factor EPAS1 is essential for catecholamine homeostasis and protection against heart failure during embryonic development. *Genes Dev.* **12**, 3320–3324 (1998).
21. Scortegagna, M. *et al.* Multiple organ pathology, metabolic abnormalities and impaired homeostasis of reactive oxygen species in *Epas1*$^{-/-}$ mice. *Nat. Genet.* **35**, 331–340 (2003).
22. Komori, T. Regulation of skeletal development by the Runx family of transcription factors. *J. Cell. Biochem.* **95**, 445–453 (2005).
23. Arnold, M.A. *et al.* MEF2C transcription factor controls chondrocyte hypertrophy and bone development. *Dev. Cell* **12**, 377–389 (2007).
24. Magee, C., Nurminskaya, M., Faverman, L., Galera, P. & Linsenmayer, T.F. SP3/SP1 transcription activity regulates specific expression of collagen type X in hypertrophic chondrocytes. *J. Biol. Chem.* **280**, 25331–25338 (2005).
25. Pescador, N. *et al.* Identification of a functional hypoxia-responsive element that regulates the expression of the egl nine homologue 3 (egln3/phd3) gene. *Biochem. J.* **390**, 189–197 (2005).
26. Pritzker, K.P. *et al.* Osteoarthritis cartilage histopathology: grading and staging. *Osteoarthritis Cartilage* **14**, 13–29 (2006).
27. Muraki, S. *et al.* Prevalence of radiographic knee osteoarthritis and its association with knee pain in the elderly of Japanese population–based cohorts: the ROAD study. *Osteoarthritis Cartilage* **17**, 1137–1143 (2009).
28. Li, Q. & Verma, I.M. NF-κB regulation in the immune system. *Nat. Rev. Immunol.* **2**, 725–734 (2002).
29. Stewart, A.J., Houston, B. & Farquharson, C. Elevated expression of hypoxia inducible factor-2α in terminally differentiating growth plate chondrocytes. *J. Cell. Physiol.* **206**, 435–440 (2006).
30. Amarilio, R. *et al.* HIF1α regulation of Sox9 is necessary to maintain differentiation of hypoxic prechondrogenic cells during early skeletogenesis. *Development* **134**, 3917–3928 (2007).

31. Bohensky, J. *et al.* Regulation of autophagy in human and murine cartilage: hypoxia-inducible factor 2 suppresses chondrocyte autophagy. *Arthritis Rheum.* **60**, 1406–1415 (2009).
32. Srinivas, V., Bohensky, J., Zahm, A.M. & Shapiro, I.M. Autophagy in mineralizing tissues: microenvironmental perspectives. *Cell Cycle* **8**, 391–393 (2009).
33. Gress, C.J. & Jacenko, O. Growth plate compressions and altered hematopoiesis in collagen X null mice. *J. Cell Biol.* **149**, 983–993 (2000).
34. Kwan, K.M. *et al.* Abnormal compartmentalization of cartilage matrix components in mice lacking collagen X: implications for function. *J. Cell Biol.* **136**, 459–471 (1997).
35. Rosati, R. *et al.* Normal long bone growth and development in type X collagen–null mice. *Nat. Genet.* **8**, 129–135 (1994).
36. Tamiya, H. *et al.* Analysis of the Runx2 promoter in osseous and non-osseous cells and identification of HIF2A as a potent transcription activator. *Gene* **416**, 53–60 (2008).
37. Echtermeyer, F. *et al.* Syndecan-4 regulates ADAMTS-5 activation and cartilage breakdown in osteoarthritis. *Nat. Med.* **15**, 1072–1076 (2009).
38. Glasson, S.S. *et al.* Deletion of active ADAMTS5 prevents cartilage degradation in a murine model of osteoarthritis. *Nature* **434**, 644–648 (2005).
39. Lin, A.C. *et al.* Modulating hedgehog signaling can attenuate the severity of osteoarthritis. *Nat. Med.* **15**, 1421–1425 (2009).
40. Stanton, H. *et al.* ADAMTS5 is the major aggrecanase in mouse cartilage in vivo and in vitro. *Nature* **434**, 648–652 (2005).
41. Little, C.B. *et al.* Matrix metalloproteinase 13-deficient mice are resistant to osteoarthritic cartilage erosion but not chondrocyte hypertrophy or osteophyte development. *Arthritis Rheum.* **60**, 3723–3733 (2009).
42. Iliopoulos, D., Malizos, K.N., Oikonomou, P. & Tsezou, A. Integrative microRNA and proteomic approaches identify novel osteoarthritis genes and their collaborative metabolic and inflammatory networks. *PLoS One* **3**, e3740 (2008).

ONLINE METHODS

Cell cultures. We cultured HeLa (Riken BRC), OUMS27 (the Health Science Research Resources Bank) and SW1353 (American Type Culture Collection) cells in DMEM with 10% FBS and ATDC5 cells (Riken BRC) in DMEM and F12 (1:1) with 5% FBS, and we performed experiments using these cell lines as previously described[43]. We used TNF-α and IL-1β (Peprotech) at final concentrations of 1 ng ml^{-1} for 2 d.

Construction of expression vectors. We prepared expression vectors for the luciferase assay and for co-immunoprecipitation in pCMV-HA (Clontech) and pCMV-3Tag-1A (Stratagene), respectively, and created the dnRUNX2, dnHIF-2α and HIF-2α mutants at the oxygen-dependent hydroxylation residues as previously described[13,44,45]. We constructed an siRNA vector for the mouse *Epas1* gene (nucleotides 1,140–1,160) with piGENEmU6 vector (iGENE Therapeutics)[46] and pMx vectors[47], retrovirus vectors using pMx vectors[47,48], adenovirus vectors by the AdenoX Expression system (Clontech), and we verified all vectors by DNA sequencing.

Luciferase assay. We prepared the *COL10A1* promoter region (from −1,028 to +127 bp relative to the TSS), *MMP13* (−1,000 to 0), *VEGFA* (−1,000 to 0), *RUNX2* (−1,480 to 0), *IHH* (−1,488 to 0), *PTH1R* (−1,529 to 0), *MMP3* (−1,551 to +39), *MMP9* (−1,775 to +17) and *EPAS1* (−1,000 to +488) by PCR using human genomic DNA as the template, and we cloned them into the pGL3-Basic vector or the pGL4.10[luc2] vector (Promega). We created deletion and mutation constructs by PCR, performed luciferase assays with the Dual-Luciferase Reporter Assay System (Promega) and showed the data as the ratio of the firefly activities to the *Renilla* activities.

Co-immunoprecipitation and mammalian two-hybrid assays. We performed co-immunoprecipitation with EZ view Red Protein A and anti-FLAG M2 Affinity Gels (Sigma) and mammalian two-hybrid assays with the Checkmate mammalian two-hybrid system (Promega).

Electrophoretic mobility shift assay. We prepared HIF-2α and ARNTL proteins by *in vitro* translation with the TNT T7 Quick System (Promega) and the pCITE4 vector (Novagen), and we performed the EMSA with the DIG Gel Shift Kit (Roche). Regions of the oligonucleotide probe were as follows: *COL10A1*, from +70 to +111 bp relative to the TSS; *MMP13*, −125 to −81; *VEGFA*, −1,002 to −957.

Chromatin immunoprecipitation assay. We performed the ChIP assay in SW1353 cells with a OneDay ChIP kit (Diagenode). For immunoprecipitation, we used antibodies to HIF-2α (Santa Cruz Biotechnology) and the normal rabbit IgG (Invitrogen). Primer sets, one spanning and the other not spanning the identified enhancer element, are as follows: *COL10A1*, +32 to +249 and −2,131 to −1,900; *MMP13*, −214 to −29 and −4,797 to −4,551; *VEGFA*, −1,000 to −795 and −4,685 to −4,507, respectively.

Mice. We purchased Hif-2α–mutant mice[20] from the Jackson Laboratory. In each experiment, we compared male *Epas1*$^{+/-}$ and wild-type littermates. We performed all experiments according to a protocol approved by the Animal Care and Use Committee of the University of Tokyo. We isolated primary chondrocytes from the ribs of mouse embryos, cultured them in a monolayer for 2 d and in a pellet for additional 2 weeks in DMEM with 10% FBS and transduced adenoviruses at 100 multiplicities of infection 4 h before the pellet formation.

Osteoarthritis experiment. We performed the surgical procedure to create an experimental osteoarthritis model on 8-week-old male mice as previously reported[4–6], and we analyzed them 8 weeks after surgery. We quantified osteoarthritis severity by our original grading system[4] and by the OARSI system (0–6 for grade and 0–24 for score)[26], which was assessed by a single observer who was blinded to the experimental group. We performed histomorphometric measurements in eight optical fields of the subchondral bones, according to the American Society for Bone and Mineral Research nomenclature report[49].

Human samples. We obtained human samples from individuals undergoing total knee arthroplasty after obtaining written informed consent as approved by the Ethics Committee of the University of Tokyo. We histologically assessed cartilage samples with the modified Mankin scoring system[50,51].

Case-control association study. We recruited individuals over 50 years of age with (n = 397; mean age, 75.6; range, 53–89) and without (n = 437; mean age, 73.6; range, 60–87) knee osteoarthritis in a population-based cohort of the ROAD study[27]. We diagnosed osteoarthritis on the basis of radiographic findings by the Kellgren-Lawrence grading system[52]: the knee osteoarthritis population included individuals with grades 3 and 4 and the control population with grades 0 and 1. After obtaining written informed consent as approved by the Ethics Committee of the University of Tokyo, we extracted genomic DNA from peripheral blood leukocytes of individuals using standard protocols. We searched SNPs around the *EPAS1* gene using the dbSNP database, and we genotyped the identified SNP by PCR restriction fragment length polymorphism (RFLP) using BanI as the enzyme. We confirmed that the P value of the Hardy-Weinberg equilibrium test in the control population was higher than 0.01.

Other analyses. We performed real-time RT-PCR, western blotting and histological analyses as previously reported[48,53]. Primer sequences and antibody information are available upon request.

Statistical analyses. We performed statistical analyses of experimental data with the unpaired two-tailed Student's t test. In the case control association study, we evaluated genotypic and allelic models by the χ^2 test for the Hardy-Weinberg equilibrium using spreadsheet software (Excel). P values less than 0.05 were considered significant.

43. Saito, T., Ikeda, T., Nakamura, K., Chung, U.I. & Kawaguchi, H. S100A1 and S100B, transcriptional targets of SOX trio, inhibit terminal differentiation of chondrocytes. *EMBO Rep.* **8**, 504–509 (2007).
44. Maemura, K. *et al.* Generation of a dominant-negative mutant of endothelial PAS domain protein 1 by deletion of a potent C-terminal transactivation domain. *J. Biol. Chem.* **274**, 31565–31570 (1999).
45. Ueta, C. *et al.* Skeletal malformations caused by overexpression of Cbfa1 or its dominant negative form in chondrocytes. *J. Cell Biol.* **153**, 87–100 (2001).
46. Miyagishi, M. & Taira, K. RNAi expression vectors in mammalian cells. *Methods Mol. Biol.* **252**, 483–491 (2004).
47. Kitamura, T. New experimental approaches in retrovirus-mediated expression screening. *Int. J. Hematol.* **67**, 351–359 (1998).
48. Morita, S., Kojima, T. & Kitamura, T. Plat-E: an efficient and stable system for transient packaging of retroviruses. *Gene Ther.* **7**, 1063–1066 (2000).
49. Parfitt, A.M. *et al.* Bone histomorphometry: standardization of nomenclature, symbols, and units. Report of the ASBMR Histomorphometry Nomenclature Committee. *J. Bone Miner. Res.* **2**, 595–610 (1987).
50. Mankin, H.J., Dorfman, H., Lippiello, L. & Zarins, A. Biochemical and metabolic abnormalities in articular cartilage from osteo-arthritic human hips. II. Correlation of morphology with biochemical and metabolic data. *J. Bone Joint Surg. Am.* **53**, 523–537 (1971).
51. Ostergaard, K., Andersen, C.B., Petersen, J., Bendtzen, K. & Salter, D.M. Validity of histopathological grading of articular cartilage from osteoarthritic knee joints. *Ann. Rheum. Dis.* **58**, 208–213 (1999).
52. Kellgren, J.H. & Lawrence, J.S. Radiological assessment of osteo-arthrosis. *Ann. Rheum. Dis.* **16**, 494–502 (1957).
53. Hirata, M. *et al.* C/EBPβ promotes transition from proliferation to hypertrophic differentiation of chondrocytes through transactivation of p57. *PLoS One* **4**, e4543 (2009).

Hypertension Research (2010) 33, 616–621
 0916-9636/10 $32.00
www.nature.com/hr

ORIGINAL ARTICLE

Rationale and design of the Eplerenone combination Versus conventional Agents to Lower blood pressure on Urinary Antialbuminuric Treatment Effect (EVALUATE) trial: a double-blinded randomized placebo-controlled trial to evaluate the antialbuminuric effects of an aldosterone blocker in hypertensive patients with albuminuria

Katsuyuki Ando[1], Hiroshi Ohtsu[2], Yoshihiro Arakawa[3], Kiyoshi Kubota[4], Takuhiro Yamaguchi[2], Miki Nagase[1], Akira Yamada[5] and Toshiro Fujita[1], on behalf of the EVALUATE Study Investigators

Although inhibitors of the renin–angiotensin system are effective as first-line antihypertensive drugs in hypertensive patients with chronic kidney disease, they cannot completely prevent the progression of renal injury. Many animal studies, including our own, and a few human studies suggest that mineralocorticoid receptor blockade could inhibit the ongoing renal damage in chronic kidney disease. Thus, we designed this double-blinded, randomized, placebo-controlled trial to evaluate the antialbuminuric effect of a low dose (50 mg day^{-1}) of the mineralocorticoid receptor antagonist eplerenone. The study subjects will include 340 hypertensive patients (blood pressure: 130–180/80–100 mm Hg) with albuminuria (urinary albumin/creatinine ratio: 30–600 mg g^{-1} in the first morning void urine), who are treated with an inhibitor of the renin–angiotensin system. Other classes of antihypertensive drugs may be added as needed to achieve the target blood pressure (<130/80 mm Hg). The primary study end point is the change in the urinary albumin/creatinine ratio after a 1-year study period. This trial is expected to show whether a low dose of mineralocorticoid receptor antagonists can exert an antialbuminuric effect in patients with chronic kidney disease.
Hypertension Research (2010) 33, 616–621; doi:10.1038/hr.2010.46; published online 9 April 2010

Keywords: mineralocorticoid receptor antagonist; urinary albumin; chronic kidney disease

INTRODUCTION

Chronic kidney disease (CKD) should be treated properly while it is still at an early stage because it is strongly associated with progression to both end-stage kidney disease (ESKD) and cardiovascular disease (CVD). As CKD is often associated with hypertension, which accelerates the progression of both ESKD and CVD, strict blood pressure (BP) control is essential for its management. Thus, CKD patients are usually given antihypertensive drugs. Considerable clinical evidence shows that renin–angiotensin system (RAS) inhibitors, such as angiotensin receptor blockers (ARBs) and angiotensin-converting enzyme (ACE) inhibitors, are acceptable as first-line antihypertensive agents for CKD.[1,2,3] However, they cannot completely prevent CKD progression. Thus, second-line depressor agents for CKD are needed. Currently, these treatments include calcium channel blockers (CCBs) or diuretics,[3] but the evidence supporting this approach is weak.[4,5] More effective renoprotective antihypertensive agents are required. New lines of evidence suggest that mineralocorticoid receptor (MR)-blocking agents may be suitable for this purpose.

Renoprotective effect of MR blockade

Recent studies revealed that MR antagonists have renoprotective effects. Although the infusion of aldosterone and excessive dietary salt progressively induce proteinuria and renal podocyte injury in rats, these effects are almost completely reversed by the MR antagonist

[1]Department of Nephrology and Endocrinology, Faculty of Medicine, University of Tokyo Hospital, Tokyo, Japan; [2]Department of Clinical Trial Data Management, Faculty of Medicine, University of Tokyo Hospital, Tokyo, Japan; [3]University of Tokyo Clinical Research Center, University of Tokyo Hospital, University of Tokyo, Tokyo, Japan; [4]Department of Pharmacoepidemiology, Faculty of Medicine, University of Tokyo, Tokyo, Japan and [5]First Department of Internal Medicine, Kyorin University School of Medicine, Tokyo, Japan
Correspondence: Dr T Fujita, Department of Nephrology and Endocrinology, Faculty of Medicine, University of Tokyo, 7-3-1, Hongo, Bunkyo-ku, Tokyo, 113-8655, Japan.
E-mail: fujita-dis@h.u-tokyo.ac.jp
Received 14 January 2010; accepted 9 February 2010; published online 9 April 2010

eplerenone.[6] Eplerenone also suppresses the progressive renal injury of the obese spontaneously hypertensive rats (SHR), known as SHR/NDmcr-cp, which exhibit metabolic syndrome characteristics and have high plasma aldosterone levels.[7] Importantly, eplerenone ameliorates renal injury in a low aldosterone model of CKD as well.[8] Thus, plasma aldosterone levels do not necessarily seem to reflect renal MR activity. These observations suggest that aldosterone-dependent[6,7] and/or aldosterone-independent[8–11] MR activation may have an essential role in CKD pathophysiology and that MR blockade may be an effective renoprotective strategy. Indeed, clinical studies have shown that plasma aldosterone profiles are not predictive of the antihypertensive efficacy of MR blockade.[12] Accordingly, the antialbuminuric effect of the MR blocker may also not be predicted by plasma aldosterone concentration.

Renal effects of MR blockade *vs.* RAS inhibition

In salt-loaded Dahl salt-sensitive rats, eplerenone suppresses the renal injury more effectively than the ACE inhibitor and to a similar degree as the combination of both drugs.[13] In addition, in stroke-prone spontaneously hypertensive rats (SHRSP), aldosterone infusion completely abolishes the renoprotective effect of the ACE inhibitor.[14] Thus, MR blockade may be even better than RAS-inhibiting agents at suppressing renal injury progression. Supporting this hypothesis are data indicating that RAS blockade does not ameliorate diabetic nephropathy in patients with aldosterone breakthrough (where plasma aldosterone levels again increase after long-term RAS-inhibitor treatment),[15] whereas the aldosterone antagonist, spironolactone, decreases the urinary protein levels of such patients.

Human studies of renoprotection by MR blockade

Several human studies have revealed that MR antagonists have renoprotective effects in addition to the cardioprotective action that has been already established by clinical mega-studies.[16,17] For example, eplerenone reduces the urinary albumin/creatinine (Cr) ratios in older patients with systolic hypertension and microalbuminuria much better than the CCB, amlodipine.[18] Moreover, although both eplerenone and the ACE inhibitor, enalapril, decrease urinary albumin levels in hypertensive patients with albuminuria, eplerenone has a superior antialbuminuric effect.[12] Although high doses (up to 200 mg day^{-1}) of eplerenone were used in these studies, a short duration (12 weeks) of treatment with relatively low doses (50–100 mg day^{-1}) of eplerenone has also been shown to decrease urinary albumin/Cr ratios in a small number of RAS inhibitor-treated patients with type 2 diabetic nephropathy.[19] Thus, a long-term and larger trial testing whether a low dose of eplerenone can protect the renal function of CKD patients is necessary.

Renoprotective effect of MR blockade in Japanese patients

Aldosterone induces inflammatory cell infiltration and vasculitis in the kidneys of rats in the context of excessive salt intake.[20,21] We also observed that aldosterone treatment causes proteinuria and podocyte injury in rats fed a high salt diet.[6] Furthermore, in subjects with high urinary aldosterone levels, urinary protein levels increase progressively as dietary salt levels rise.[22] Thus, the harmful effects of aldosterone on the renocardiovascular system become apparent on salt repletion.[23,24] As salt intake in Japan is high on average,[25] it may be useful to treat Japanese CKD patients with MR blockers.

Evaluation of the antialbuminuric effect of eplerenone

It is, therefore, of considerable interest to determine whether a low dose (50 mg day^{-1}) of the highly MR-specific antagonist, eplerenone, has antialbuminuric effects in hypertensive CKD patients in Japan. Consequently, we designed the double-blinded, randomized, placebo-controlled Eplerenone combination Versus conventional Agents to Lower blood pressure on Urinary Antialbuminuric Treatment Effect (EVALUATE) trial to compare the antialbuminuric effect between a 50-mg day^{-1} eplerenone dose and placebo.

Hypothesis and objectives. Our hypothesis is that the MR blockade induced by a low dose of eplerenone effectively suppresses renal injury progression in RAS inhibitor-treated CKD patients. The primary trial objective is to compare the antialbuminuric effects of a 1-year treatment with eplerenone or placebo. Key secondary objectives are: (1) to compare eplerenone- and placebo-treated patients in terms of changes in serum Cr levels, estimated glomerular filtration rate (eGFR) and urinary liver-type free fatty acid-binding protein levels (L-FABP; an early marker of tubulointerstitial stress)[26,27] and (2) to determine the effect of high salt intake on the putative renoprotective effects of eplerenone.

METHODS

End points

Primary end point. This end point refers to the percent change in the urinary albumin/Cr ratio in the first morning void urine after 12 treatment months relative to the pretreatment ratio (an average of three continuously measured values). Urinary albumin and Cr levels will be measured by immunoturbidimetrical (autoanalyzer: JCA-BM8000 series, JEOL, Tokyo, Japan) and enzymatic (JCA-BM8000 series, JEOL) methods, respectively.

Secondary end points. These end points are the absolute values and percent changes at each treatment period relative to the pretreatment values of urinary albumin/Cr ratio (4, 8, 28 and 52 weeks after the start of the trial drugs) in the first morning void urine, serum Cr levels, eGFR, urinary L-FABP levels and office BP. The secondary end points also include the estimated 24-h urinary sodium (Na) excretion, plasma aldosterone concentration, urinary aldosterone and cerebro-cardiovascular events. We will evaluate whether the estimated urinary Na excretion and baseline plasma aldosterone correlate to the degree of the antialbuminuric effect of eplerenone. eGFR will be calculated using the 'Modified Diet in Renal Disease (MDRD) formula' modified by the Japanese Society of Nephrology.[28] Urinary L-FABP will be measured by an enzyme-linked immunosorbent assay (ELISA: Human L-FABP Assay Kit-IBL: Immuno-Biological Laboratories, Takasaki, Japan). Urinary Na excretion over a day will be estimated by a previously reported formula.[29,30] Cerebro-cardiovascular events include cerebro-cardiovascular death (fatal myocardial infarction, fatal heart failure, sudden death, fatal stroke and other cardiovascular deaths) and hospitalization due to cerebro-cardiovascular disease (nonfatal myocardial infarction, angina, heart failure, cerebral bleeding, cerebral infarction and transient cerebral ischemic attack).

Other end points. The safety of the eplerenone treatment will be determined by measuring serum potassium (K) changes and adverse events.

Study design

The double-blinded, randomized, placebo-controlled EVALUATE trial will compare the changes in urinary albumin/Cr ratio of eplerenone- and placebo-treated, hypertensive, RAS inhibitor-treated patients with albuminuria (Figure 1). During each initial screening visit, written informed patient consent will be obtained, interim registration will be performed and all examinations except for urinalysis will be conducted to evaluate patient eligibility, and three urine-sampling kit sets (Uro Catch II, Atleta, Osaka, Japan) for sampling the first morning void urine will be provided. On the second visit, the patient will bring these urine samples. After confirming patient eligibility, each patient will be officially registered and randomly allocated into a 50-mg day^{-1} eplerenone group or a placebo group. The following factors will be used for stratified randomization: urinary albumin/Cr ratio (<300 mg, $\geqslant 300$ mg g^{-1}); systolic BP (<140 mm Hg and $\geqslant 140$ mm Hg); and usage of a particular RAS inhibitor

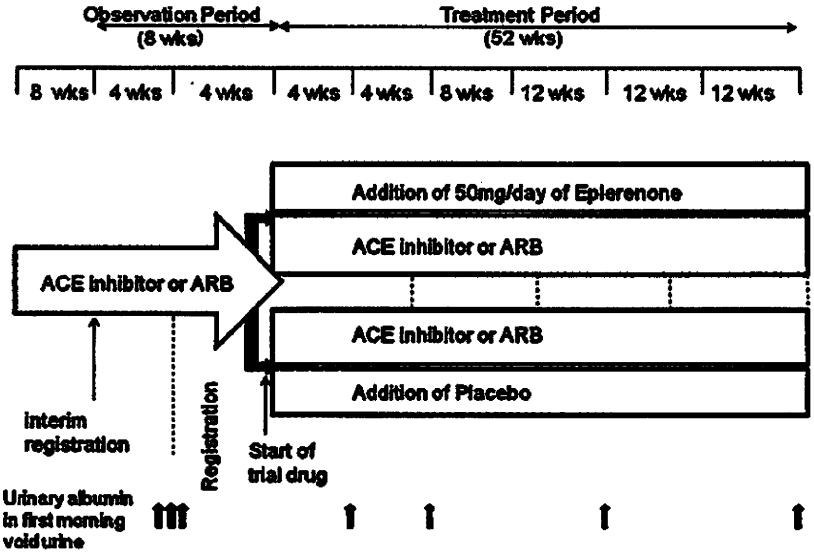

Figure 1 Design of the Eplerenone combination Versus conventional Agents to Lower blood pressure on Urinary Antialbuminuric Treatment Effect (EVALUATE) Trial. ACE inhibitor: angiotensin converting enzyme inhibitor; ARB: angiotensin receptor blocker; wks: weeks. During the trial period, if blood pressure (BP) does not reach <130/80 mm Hg, an antihypertensive drug other than mineralocorticoid receptor antagonists and renin–angiotensin system inhibitors will be added.

class (ACE inhibitor, ARB orACE inhibitor plus ARB). Thereafter, eplerenone or placebo (both blinded by encapsulation (DBcaps: Capsugel Japan, Sagamihara, Japan)) will be started (together with the RAS inhibitors that will have been given for more than 16 weeks). To ensure that any placebo-treated patients who develop high BP and any eplerenone-treated patients who develop hyperkalemia are promptly treated, the BP and serum K levels of all patients will be assessed 4 weeks after the trial drug is started. Thereafter, the patients will visit the clinic 8, 16, 28, 40 and 52 weeks after commencing treatment. All prior antihypertensive therapies will continue. If BP does not drop to <130/80 mm Hg, an antihypertensive drug other than MR antagonists and RAS inhibitors will be added.

Study subjects

Patients to be enrolled in the EVALUATE trial will be hypertensive RAS inhibitor-treated patients with albuminuria who satisfy the following inclusion and exclusion criteria.

Inclusion criteria. The inclusion criteria are: age ⩾20 year and <80 year; outpatient systolic BP ⩾130 and <180 mm Hg and/or diastolic BP ⩾80 and <100 mm Hg; pretreatment urinary albumin/Cr ratio in the first morning void urine (an average of three continuously measured values) ⩾30 and <600 mg g^{-1}; eGFR ⩾50 ml min^{-1} 1.73 m^{-2}; ACE inhibitor and/or ARB administered for ⩾8 weeks at interim registration.

Exclusion criteria. Hypertensive emergencies that require intravenous administration of antihypertensives; serum K ⩾5.0 mEq l^{-1}; diabetes (fasting blood glucose ⩾126 mg 100 ml^{-1} or treatment with an antidiabetic drug); severe liver damage (Child–Pugh Score: class C); severe heart failure (New York Heart Association (NYHA) class ⩾III); severe arrhythmia (frequent ventricular or atrial extrasystoles, prolonged ventricular tachycardia, atrial tachyrhythmia with severe tachycardia, atrial fibrillation or flutter with severe tachycardia, sick sinus syndrome with severe bradycardia, atrio-ventricular block with severe bradycardia); angina; myocardial infarction and cerebrovascular disease if they occurred <6 months before the interim registration; pregnancy, possibility of pregnancy, desire to become pregnant; a past history of severe side effects from MR antagonists, ACE inhibitors or ARBs; an MR antagonist administered <8 weeks before the interim registration; contraindicated drugs, including adrenocorticosteroidal drugs, immunosuppressants, K-sparing diuretics, K supplementation, itraconazole, ritonavir and nelfinavir; treatment for >2 weeks with non-steroid anti-inflammatory drugs (NSAIDs).

Statistical considerations and study size

Sample size determination. As RAS-inhibitor treatment of hypertensive patients with albuminuria decreases urinary albumin levels by 45%, whereas RAS inhibitor plus eplerenone decreases it by 74%,[31] it is estimated that eplerenone will decrease urinary albumin levels of RAS inhibitor-treated patients by 30% (that is, an effect size of 30%). In addition, estimates are within a s.d. value of the albumin/Cr ratio in the first morning void urine of 90%, a statistical power of 80%, and a dropout rate of 10%. Thus, to compare the eplerenone and placebo groups at a two-sided overall significance level of 5% with regard to the primary efficacy end point, 340 patients (170 patients for each group) will be required.

Statistical analysis. For the efficacy end point, the primary analysis will be carried out on the intent-to-treat (ITT) population (that is, all randomized patients, regardless of patient compliance, actual administration of the trial drug or premature trial drug discontinuation), not including patients deemed ineligible (see eligibility criteria above) or who never take the trial drug. In terms of the safety end point, all patients who take the trial drug will be analyzed.

The eplerenone and placebo groups will be compared in terms of the percentage change in the urinary albumin/Cr ratio after 12 months of treatment relative to the pretreatment ratio by using an unpaired *t*-test at a two-sided significance level of 5%. If necessary, the data will be adjusted by important background factors, including gender, age, BP response to the treatment, eGFR level, urinary L-FABP levels and urinary Na excretion. In addition, analysis with a linear model will be performed for percent changes in the urinary albumin/Cr ratio from the pretreatment period to each point of treatment, in the absolute value of urinary albumin/Cr ratio, and for their time-dependent changes. The absolute values and changes over time of the following parameters will also be analyzed: urinary L-FABP level, office BP, eGFR level, estimated Na excretion over a day and plasma aldosterone concentration. The groups will also be compared in terms of the rate of CKD stage progression, all-cause mortality and frequency of cardiovascular events (cerebro-cardiovascular death (fatal myocardial infarction, fatal heart failure, sudden death, fatal stroke and other cardiovascular death) and hospitalization due to cerebro-cardiovascular events (non-fatal myocardial infarction, angina, heart failure, cerebral